



Escola d'Enginyeria de Telecomunicació i  
Aeroespacial de Castelldefels

UNIVERSITAT POLITÈCNICA DE CATALUNYA

# TREBALL DE FI DE CARRERA

**TÍTOL DEL TFC: Estudi de dinàmica de fluids computacional d'una cometa de kitesurf**

**TITULACIÓ: Enginyeria Tècnica Aeronàutica, especialitat Aeronavegació**

**AUTOR: Inglés Sala, Andrea**

**DIRECTOR: Villardi de Montlaur, Adeline de**

**DATA: 14/07/2012**



**Títol:** Estudi de dinàmica de fluids computacional d'una cometa de kitesurf

**Autor:** Inglés Sala, Andrea

**Director:** Villardi de Montlaur, Adeline de

**Data:** 14/07/2012

## Resum

El kitesurf és un esport que consisteix en surfejar utilitzant una cometa especialment dissenyada com a propulsió; gràcies a la força del vent. Tant en el camp de la investigació com per la indústria del kitesurf, l'aerodinàmica del kite és un punt crucial. Aquest treball intenta explicar alguns aspectes bàsics d'aquest per un model específic en una situació estacionària depenent de tres variables: l'angle d'atac, l'angle d'inclinació i la intensitat del vent.

Utilitzant el software Ansys, s'ha fet un anàlisi computacional de les forces aerodinàmiques actuant en un kite. Més tard, s'ha observat com aquests resultats afecten al kiter.

En primer lloc, s'ha vist que hi ha una diferència entre les forces actuant en un kite o en un perfil aerodinàmic. S'ha arribat a la conclusió que devia ser per la combinació del fet d'anar perpendicular al vent i per la curvatura del caire d'entrada. S'explica la variació d'aquestes forces segons les variables. I a més a més, en aquest treball es justifica perquè les cometes "bow" poden obtenir més potencia que les "C". Això és degut només a que una d'elles té més superfície orientada cap amunt.

Més tard, s'ha analitzat com les forces obtingudes en les simulacions afectaven el kiter. Amb aquest objectiu, s'han tingut en compte diferents límits sobre aquestes forces. S'ha buscat la configuració d'angles que provoca la millor operació amb un baix angle d'atac per casi tots els angles d'inclinació. A més, s'ha trobat que les velocitats escollides de vent no afecten a l'hora d'escollir la configuració.

**Title:** Computational Fluid Dynamics study of a kitesurf

**Author:** Inglés Sala, Andrea

**Director:** Villardi de Montlaur, Adeline de

**Date:** 14/07/2012

## Overview

Kitesurf is a sport of surfing while holding on to a specially designed kite, using the wind for propulsion. In the field of investigation or kitesurf industry, the kite aerodynamics is a crucial point. This work tries to explain the basic aerodynamic aspects of a specific kite model in a stationary situation depending on three variables: the angle of attack, the inclination angle and the intensity of wind.

Using the Ansys software, a computational fluid dynamics analysis of the aerodynamic forces acting on the kite has been done. After, the forces affecting the kiter are studied.

First, a difference in aerodynamic forces acting upon this kite and a common airfoil has been seen. It has been concluded that the special combination of a movement perpendicular to the wind and the curvature of the leading edge must be the reason of this difference. The variation on the forces depending on the variables is explained. And besides, it is justified why the bow kites can generate more power than C-kites. It is only a matter of which of them has more area oriented upwards.

After, the effect of the previous results on the kiter has been analyzed. For this reason, some limits have been taken into account for the different forces. The configuration of angles that cause the best performance is a low angle of attack for almost any of inclination angles. In addition, the studies show that the selected wind speed doesn't affect the choice of configuration.

# ÍNDEX

<b>INTRODUCTION</b> .....	<b>1</b>
<b>CHAPTER 1. THE KITE</b> .....	<b>4</b>
1.1. Model .....	4
1.2. Measures .....	6
1.3. Materials .....	8
<b>CHAPTER 2. ANALYSIS OF THE STATIONARY SITUATION</b> .....	<b>9</b>
2.1. Overview of the situation .....	9
2.2 Kite speed and wind speed .....	11
2.3 Controlling kite power.....	11
2.4 Effect of the angle of attack and the angle of inclination in kite power and kiter's balance. ....	14
<b>CHAPTER 3. SIMULATION APPROACH</b> .....	<b>17</b>
3.1 Geometry .....	17
3.2 Mesh.....	18
3.3 Setup.....	19
3.4 Solution .....	20
<b>CHAPTER 4. RESULTS</b> .....	<b>23</b>
4.1 Data obtained .....	23
4.2 Aerodynamic behaviour analysis .....	24
4.2.1 Lift .....	25
4.2.2 Fx .....	27
4.2.3 Lift i Fx .....	29
4.2.4 Fz .....	31
4.3 Analysis of the forces applied to the kiter .....	34
4.3.1 Force in X''-axis (Tx'') .....	34
4.3.2 Force in Y''-axis (Ty'') .....	36
4.3.3 Force in Z''-axis (Tz'') .....	38
4.3.4 Forces optimization .....	40
<b>CHAPTER 5. CONCLUSIONS</b> .....	<b>41</b>
<b>CHAPTER 6. BILIOGRAPHY</b> .....	<b>43</b>

Figure 1. Bow kites have a much flatter span than the C-kites causing more lift upwards [7].	4
Figure 2. Sled kite	5
Figure 3. Profile of the kite in the symmetric plane.	5
Figure 4. Aspect ratio	6
Figure 5. Swept back wing tips	7
Figure 6. Measure the lengths of the foil between supports.	8
Figure 7. Velocity and force basic scheme	9
Figure 8. Velocity and forces scheme in the upwind case.	10
Figure 9. Available range of wind depending on deflated area of the kite [16].	11
Figure 10. Kite's angle of attack (relation between XYZ coordinate system and X''Y''Z'' coordinate system)	12
Figure 11. Kite's inclination angle (relation between X'Y'Z' coordinate system and X''Y''Z'' coordinate system)	12
Figure 12. Kite lines scheme [18]	13
Figure 13. Vector forces decomposition.	14
Figure 14. Forces scheme	15
Figure 15. Geometry	18
Figure 16. Section of the domain.	19
Figure 17. Definition of the inlet surface (left image is for a low $\alpha$ and right for a high one).	19
Figure 18. Zenith point of the kite, where the velocity is evaluated.	20
Figure 19. Momentum and massa residues ( $\alpha=30^\circ$ , $\theta=50^\circ$ , wind speed =12 m/s )	21
Figure 20. Turbulence residues ( $\alpha=30^\circ$ , $\theta=50^\circ$ , wind speed =12 m/s )	22
Figure 21. User's point residues ( $\alpha=30^\circ$ , $\theta=50^\circ$ , wind speed =12 m/s )	22
Figure 22. Velocity contour ( $\alpha=30^\circ$ , $\theta=50^\circ$ , wind speed =12 m/s )	23
Figure 23. Pressure contour ( $\alpha=30^\circ$ , $\theta=50^\circ$ , wind speed =12 m/s )	24
Figure 24. Lift expression ( $\alpha=30^\circ$ , $\theta=50^\circ$ , wind speed =12 m/s )	24
Figure 25. Lift depending on $\alpha$ for different $\theta$ (wind speed = 10 m/s).	25
Figure 26. Lift depending on $\alpha$ for different $\theta$ (wind speed = 12m /s).	26
Figure 27. Wind window	26
Figure 28. Table of Fx comparison depending on $\theta$	27
Figure 29. Pressure distribution around the kite ( $\alpha$ is $60^\circ$ , $\theta$ is $30^\circ$ and wind speed is 10 m/s)	28
Figure 30. Fx depending on $\alpha$ and $\theta$ (wind speed = 10 m/s)	28
Figure 31. Fx depending on $\alpha$ and $\theta$ (wind speed = 12 m/s)	29
Figure 32. Resultant force (Fp) of lift and Fx (wind speed= 10 m/s).	30
Figure 33. Resultant force (Fp) of lift and Fx (wind speed=12 m/s).	30
Figure 34. Table comparing the module of Fp with respect to lift.	31
Figure 35. Table comparing the angle of Fp with respect to the lift	31
Figure 36. Fz depending on $\alpha$ and $\theta$ (wind speed = 10 m/s)	32
Figure 37. Fz depending on $\alpha$ and $\theta$ (wind speed = 12 m/s)	32
Figure 38. Pressure contour of the YZ Plane, x= 0 m ( figures in the first row have $\alpha=30^\circ$ and the second row $\alpha=45^\circ$ , starting from the left thetha increases from $0^\circ$ to $90^\circ$ )	33
Figure 39. Velocity contours of the YZ Plane, x=0 m (figure in the first row have $\theta=0^\circ$ and in the second row $\theta=90^\circ$ , the first column $\alpha=30^\circ$ and the second $\alpha=45^\circ$ ).	34

Figure 40. Components of $T_x''$ depending on $\alpha$ (wind speed = 10 m/s) .....	35
Figure 41. $T_x''$ depending on $\alpha$ and $\theta$ (wind speed = 10 m/s).....	35
Figure 42. $T_x''$ depending on $\alpha$ and $\theta$ (wind speed = 12 m/s).....	36
Figure 43. Components of $T_y''$ depending on $\alpha$ (wind speed = 10 m/s) .....	37
Figure 44. $T_y''$ depending on $\alpha$ and $\theta$ (wind speed = 10 m/s).....	37
Figure 45. $T_y''$ depending on $\alpha$ and $\theta$ (wind speed = 12 m/s).....	38
Figure 46. $T_z''$ depending on $\alpha$ and $\theta$ (wind speed = 10 m/s).....	39
Figure 47. $T_z''$ depending on $\alpha$ and $\theta$ (wind speed = 12 m/s).....	39
Figure 48. Resume table of possible configurations.....	40



## INTRODUCTION

The origin of kitesurf may be considered to be in October 1977 when a Dutch inventor, called Gijsbertus Adrianus Panhuise, was granted the first patent on this sport. The following year, the North American Dave Culp designed the first kite with an inflatable angle of attack [1].

But, what is a kite? According to “An Engineering Methodology for Kite Design” written by Breukels, J. a kite is defined as follows [2]:

*“A kite is a tethered heavier-than-air device which is able to achieve flight by generating a resulting aerodynamic force which is countered by the mass of the device and the tension force in the tether.”*

So, what is kitesurfing, also known as kiteboarding or kitesurf? In accordance with Oxford Dictionary [3], the definition of kitesurfing is the following:

*“The sport or pastime of riding on a modified surfboard while holding on to a specially designed kite, using the wind for propulsion.”*

And the person who practises this sport is called kiter, kitesurfer or kiteboarder. Despite its young history, kitesurf has been evolving really quickly and has been spreading around the world. The British Kitesurfing Association estimates at about 100,000 in 2006 in the entire world and this number is constantly growing [4]. The North American kitesurf magazine, SBC Kiteboard, assured that an industry analyst projected in 2008 a growth of kitesurfing participation to 35 % or 50 % per year [5].

The last news from this sport is that it will debut as an Olympic sport in Río de Janeiro 2016 with the modality of course racing.

Besides, kite aerodynamics is also important for this sport as a possible future energy source. Nowadays there are many investigations in that field [6].

This project tries to explain basic aspects about kite aerodynamic behaviour in a stationary situation. It focuses on the characterization of a kite model and its results. In the future, if the procedure explained here is repeated with another kite it will be possible to compare the results obtained and see which differences appear in kite aerodynamic behaviour.

The proposal of this work is to compute the lift and drag of a kite model depending on three variables. Two of the variables are the angle of attack and the inclination angle which the kitesurfer controls constantly and the other is the intensity of wind. The module of CFX in the Ansys software will be used to model the kite in 3D, mesh it, introduce the boundary conditions and, finally, analyse its aerodynamic behaviour.

The basic hypothesis is that the kite is a rigid body. Considering that the analysis is will be in a stationary situation, the variables that could have

changed its form will be constant and the intensity of the wind is supposed to be enough to inflate completely the kite.

This work is structured in 5 chapters. In the first chapter, all the basic information relative to the object of study, the kite, is explained. This chapter is divided in three subsections. The first of them introduces the types of kites and it gives a frame of reference for the model that will be studied. After, there is an explanation of which measures were taken to model the 3D kite. The last subsection is a quick view of the materials that are commonly used in kite's production. Chapter 2 is the analysis of the stationary situation. It expounds the basic knowledge of how kites can surf. Besides, the three variables that will be analysed are introduced. Afterwards, in chapter 3 all the previous information is applied to the different steps of the simulation process. Subsequently, chapter 4 is the analysis of the results and, finally, the last chapter summarizes the main results and recommendations which are obtained through this work.



## CHAPTER 1. THE KITE

### 1.1. Model

Depending on the structure, kites are classified as: C-kites, bow kites and sled kites.

The advantage of C-kites is their easy control. Moreover, bow kites are more stable and have more lift upwards as it can be seen in figure 1.

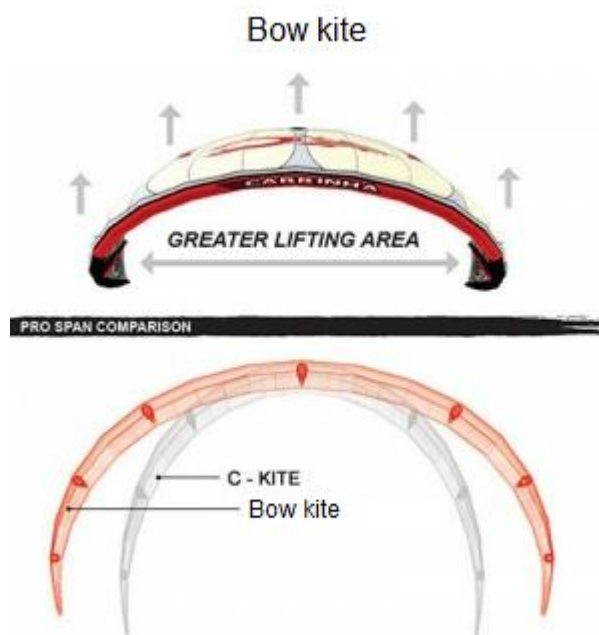


**Figure 1. Bow kites have a much flatter span than the C-kites causing more lift upwards [7].**

The similarity between C-kites and bow kites is that both consist of an inflatable leading edge, a foil that gives the curvature of the profile along all the leading edge, and inflatable supports that provide the stiffness needed. On the contrary, the sled kite is completely different, as shown in figure 2. It consists of ram-air inflated chambers. This type of structure was patented by Domina Jalbert [8] and is composed of a group of cells that let the air pass through the kite parallel to the chord. Doing so, the air outflow can be controlled by the kiter [9].



**Figure 2. Sled kite**

In this analysis, the chosen model is a bow kite, particularly, a 10 m Vertigo 2009 from the “Blade” brand. This means that kite’s area is  $10 \text{ m}^2$  when it is deflated. Some other measures of this kite can be seen in figures 3 and 4. They are shown using the 3D model that will be explained in more details in chapter 3.

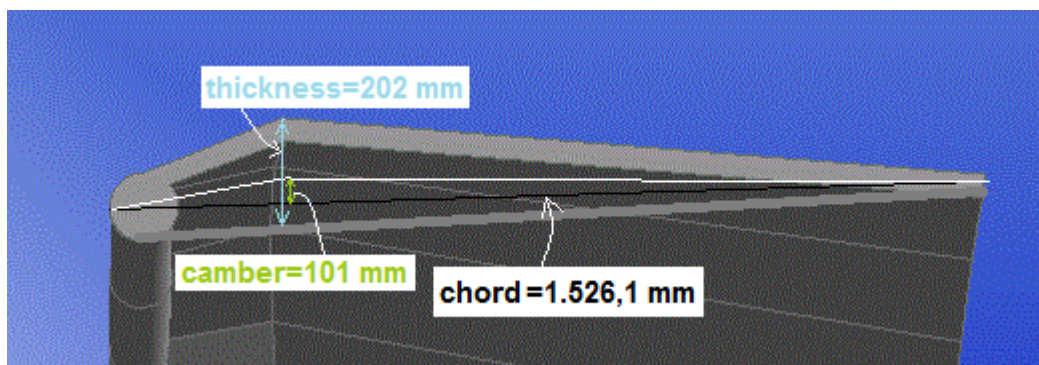


**Figure 3. Profile of the kite in the symmetric plane.**

Figure 3 shows how similar a kite is to a common airfoil. This figure make possible to compare the curvature of the supper surface of them. The main difference of a kite, when compared to a plane’s wing, is the curvature of the leading edge.

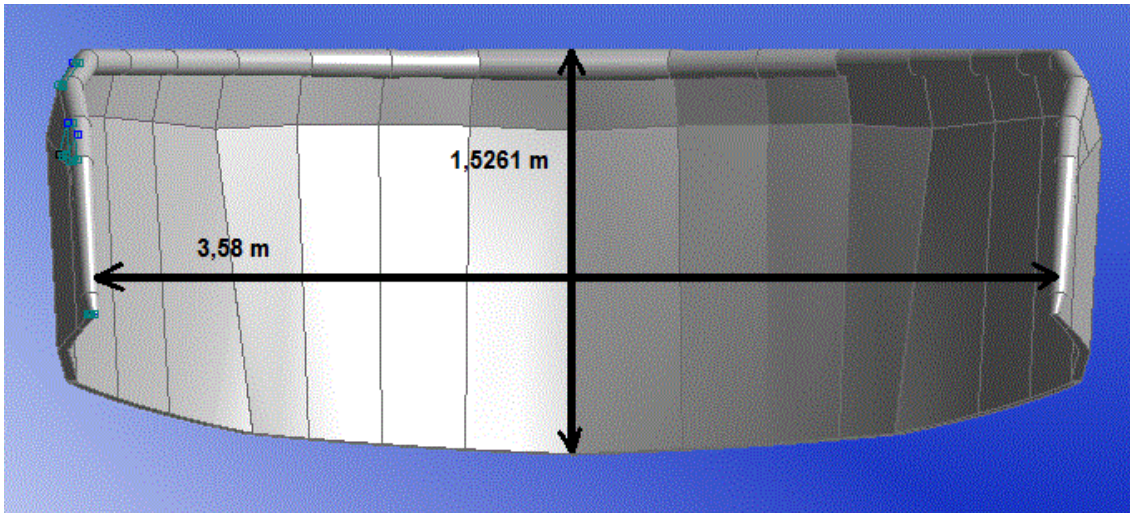


**Figure 4. Aspect ratio**

Figure 3 corresponds to a computation of the aspect ratio that in this case is:

$$AR = \frac{3,58}{1,5261} = 2.35. \quad (1.1)$$

## 1.2. Measures

The 3D process consists in 3 phases: take measures, create the 3D with DesignModeler and simplify it to avoid problems. In this section, the first phase is explained.

Due to its flexibility the kite can change its shape. The measures are taken to represent the most inflated case. It is easier to take the measures; if it was half inflated, it can change form meanwhile the measures are taken. Besides, the wind selected is supposed to be enough to provide the maximum kite's power.

The kite form is simplified and consists of a main inflatable tube and a foil. The first one corresponds to the leading edge, and the second starts in the leading edge, follows the curvature in each kite's profile and ends in the trailing edge. In addition to these main parts, a singularity of bow kite called swept back wing tips is also considered. This particularity is the curve of the leading edge in the ZY Plane, as seen in figure 5. Finally, the inflatable supports are neglected. The main objective of this support is to give stiffness to the kite. For this reason and due to the fact that the foil of the kite is supposed to have more thickness than in the reality, there would be no much difference in the aerodynamic behaviour adding or not these supports.

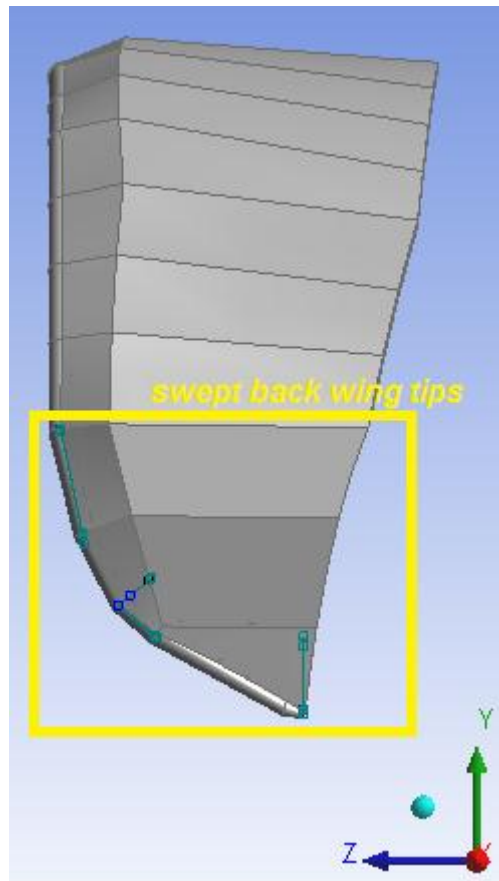


**Figure 5. Swept back wing tips**

In order to know the shape of the main inflatable tube, the measures of the curvature in the XY Plane and the diameters in each seam are taken. The foil profiles are determined in each inflatable support because the shape doesn't change there. Eventually, the lengths of the foil between inflatable supports are checked to know how much the foil could be inflated. Figure 6 is a photo taken when these lengths are measured.



Figure 6. Measure the lengths of the foil between supports.

### 1.3. Materials

To determine the drag on the kite, the type of material must be known. After some research, it is concluded that ripstop clothes are used for the foil and Dacron for the inflatable tube. The main ripstop clothes are from nylon and polyester.

Nylon ripstop is the lightest of the three materials,  $30\text{-}50\text{ gr/m}^2$ , and it is the most popular with ram air structures. Polyester ripstop is heavier than nylon ripstop,  $50\text{ gr/m}^2$ , but it has the best stress-tension relation apart from better absorption properties from the surroundings. This material is the most used for the inflatable kites foils. Finally, Dacron is a material made with Polyester too, but heavier than the other ones,  $170\text{ gr/m}^2$ . It is used in the part more affected by the sand and salt environment because it is more resistant than Polyester ripstop [10] [11].

Knowing from which type of material a kite is made, it can be concluded that the friction coefficient will be low [12].

## CHAPTER 2. ANALYSIS OF THE STATIONARY SITUATION

### 2.1. Overview of the situation

The basic question that someone asks when they first see this sport is: “How do kites use the wind to sail?” And I would add: “How do kites achieve the stationary situation?”

The answer to the first question is that the movement of the kite is mainly perpendicular to the wind (wind X’). This movement is needed to inflate the kite and the movement relative wind is in the opposite direction of the kite speed (speed Z’’) as shown in figure 7. Figure 7 shows the vectors applied to the kiter in the X’’Y’’Z’’ coordinate system, whereas the vectors applied to the kite in the XYZ coordinate system. At the top, the change in coordinate systems is shown.

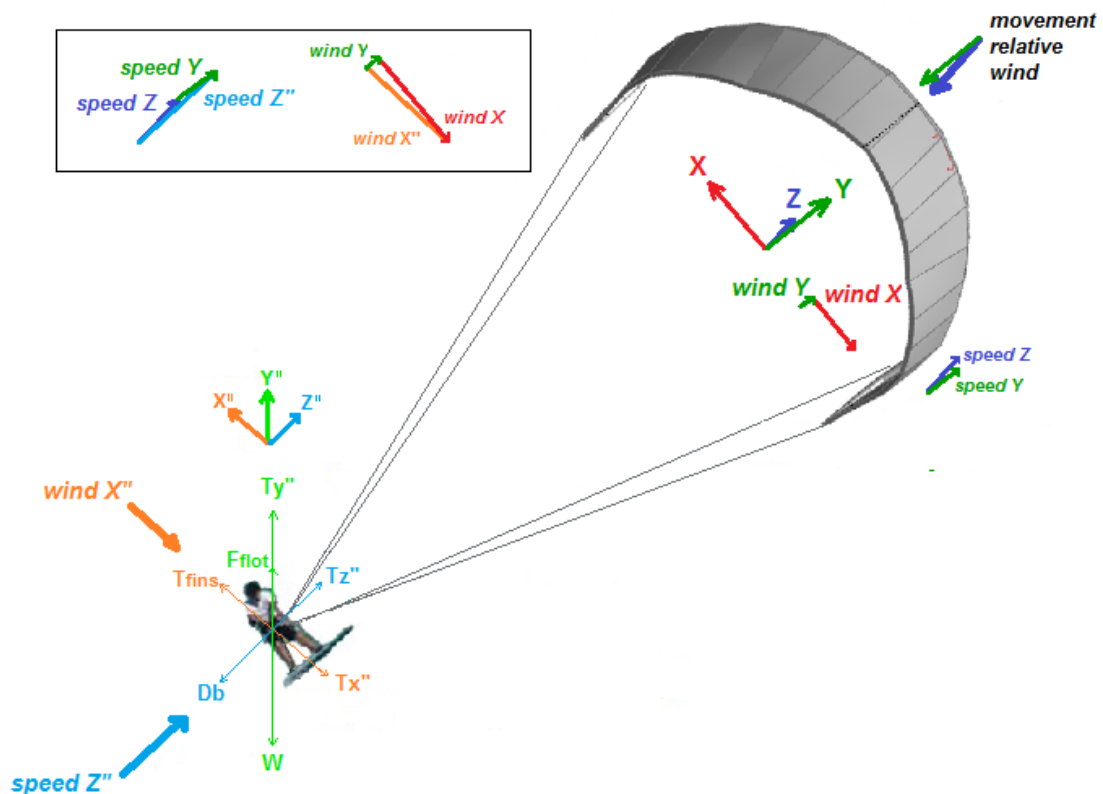


Figure 7. Velocity and force basic scheme

To achieve the stationary situation, there has to be equilibrium between the forces acting on the system in each axis, as seen in the previous figure. The analysis is done upon the kiter because the X’’Y’’Z’’ coordinate system is static. And the forces acting on him are supposed to be concentrated at a point.

On the  $Y''$ -axis, the weight of the kite and kiter ( $W$ ) is balanced, by the sum of the flotation force of the board ( $F_{\text{flot}}$ ) and the component of the kite force  $T_{y''}$  produced by the own velocity of the system. On the  $X''$ -axis, the component of the kite force  $T_{x''}$  pulls the kiter in the same direction of the wind. But not to be drag along that direction, the kiter opposes using the board's fins ( $T_{\text{fins}}$ ) and his body. Remember that a fin is a thin, usually curved projection attached to the rear bottom of a surfboard for stability [13]. Furthermore, these fins provide grip to control the kiter's trajectory [14]. On the  $Z''$ -axis, the component of the kite force  $T_{z''}$  is balanced with the drag of the board ( $D_b$ ) to be considered in a stationary situation.

However, sometimes there is a little change in forces when the kite has a deviation in the trajectory and does not go perpendicular to the wind. This happens when kites get too much or not enough speed and this situation is called going upwind or drifting, respectively. In this case, there is a component of the wind in  $Z''$ -axis. In figure 8, the kite is going upwind.

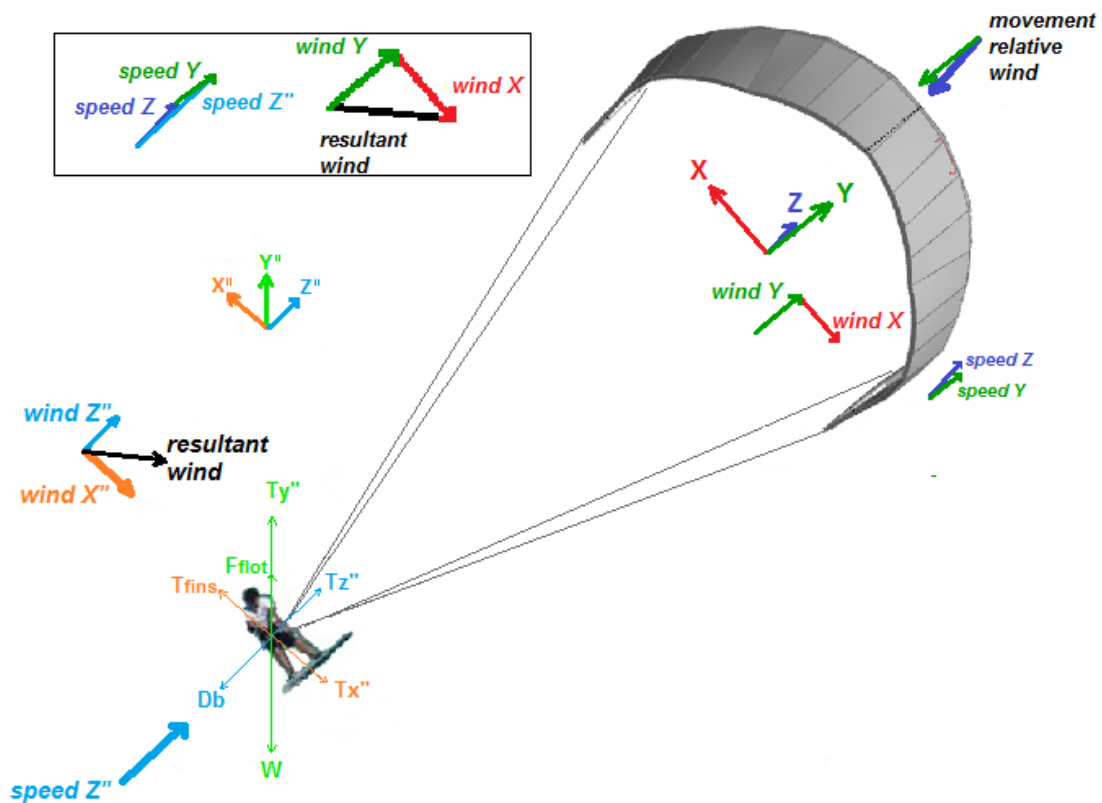


Figure 8. Velocity and forces scheme in the upwind case.

Now on the  $Y$ -axis, the kite has a bigger contribution of the wind in  $Y$ -axis that reduce the sum of the movement relative wind and the resultant wind in this axis. This effect is totally understandable, because the kiter needs more speed ( $speed\ Z''$ ) to go upwind. Instead, if the kite drifts, the kite speed is higher. Therefore, the kite will gain enough velocity to be in a stationary situation.

## 2.2 Kite speed and wind speed

Now that the basic notion of relative wind direction is understood, *which intensity does it have?*

To answer this question, we have to trust the common knowledge [15] that states that the value of the ratio between the kite speed and the wind speed is around 1.5.

The velocity range of non-perturbed wind where kites can sail is comprised around 5 kt and 40 kt. It depends on a lot of variables such as the manufacturer, the kite's wingspan, the kiter's weight and his expertise, the board used and water conditions.

According to the manual applicable to our model, which is Blade 2009, and assuming that the kiter is not a beginner, the table that relates the appropriate wind range with the kite's deflated area is shown in figure 9.

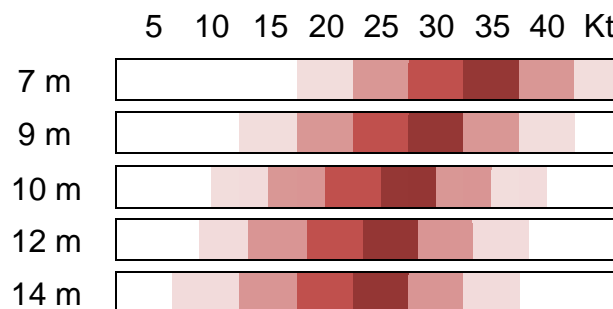


Figure 9. Available range of wind depending on deflated area of the kite [16].

Based on that, for a 10 m<sup>2</sup> deflated area of the kite the wind range can be considered around 14 kt and 33 kt. In international units, this means around 7m/s to 17 m/s.

## 2.3 Controlling kite power

The next logic question could be: *“How can kites control kite power?”*

The angle of attack and inclination angle are used to constantly control the power using the bar. These angles are the ones seen in figure 10 and 11. Further on, the change of these angles with the bar will be explained in detail.

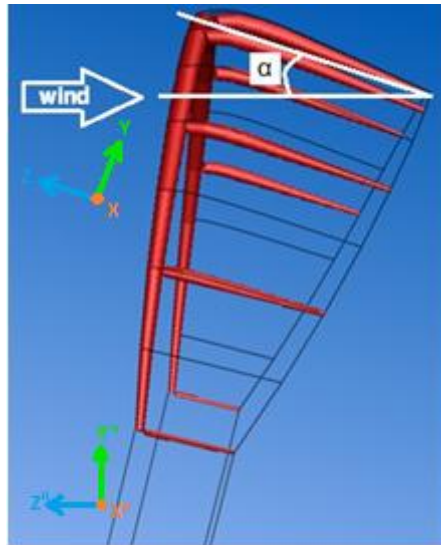


Figure 10. Kite's angle of attack (relation between XYZ coordinate system and X''Y''Z'' coordinate system)

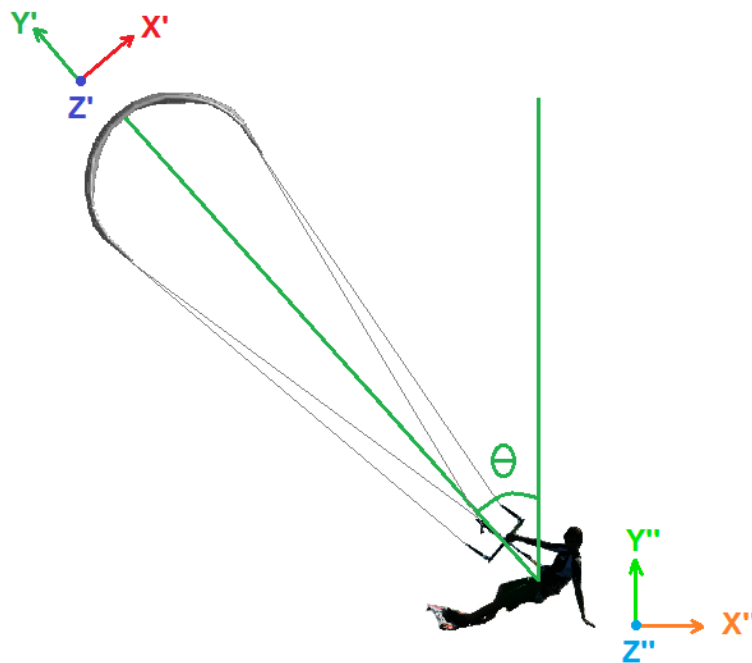


Figure 11. Kite's inclination angle (relation between X'Y'Z' coordinate system and X''Y''Z'' coordinate system)

The angle of attack  $\alpha$  of any airfoil is: the angle between the chord and the relative wind, and affects significantly the lift generated [17].

The inclination angle  $\theta$  in this project is defined as the angle between the bisector of the bar lines and the vertical line.

Before, it was commented that  $\alpha$  and the  $\theta$  can be controlled by the kiter. These angles are controlled using the inclination and position of the bar.

Figure 12 shows how the front lines are bounded to the kiter's harness, whereas the back lines are bounded to the extreme of the bar. In this manner, the kiter can pull or push symmetrically the lines by pulling or pushing the bar. Consequently, the angle of attack will increase or decrease, respectively. The change in the inclination angle will be controlled by the position given to the bar with respect to the water surface. This position of the bar is produced moving the bar with both hands to the desired position.

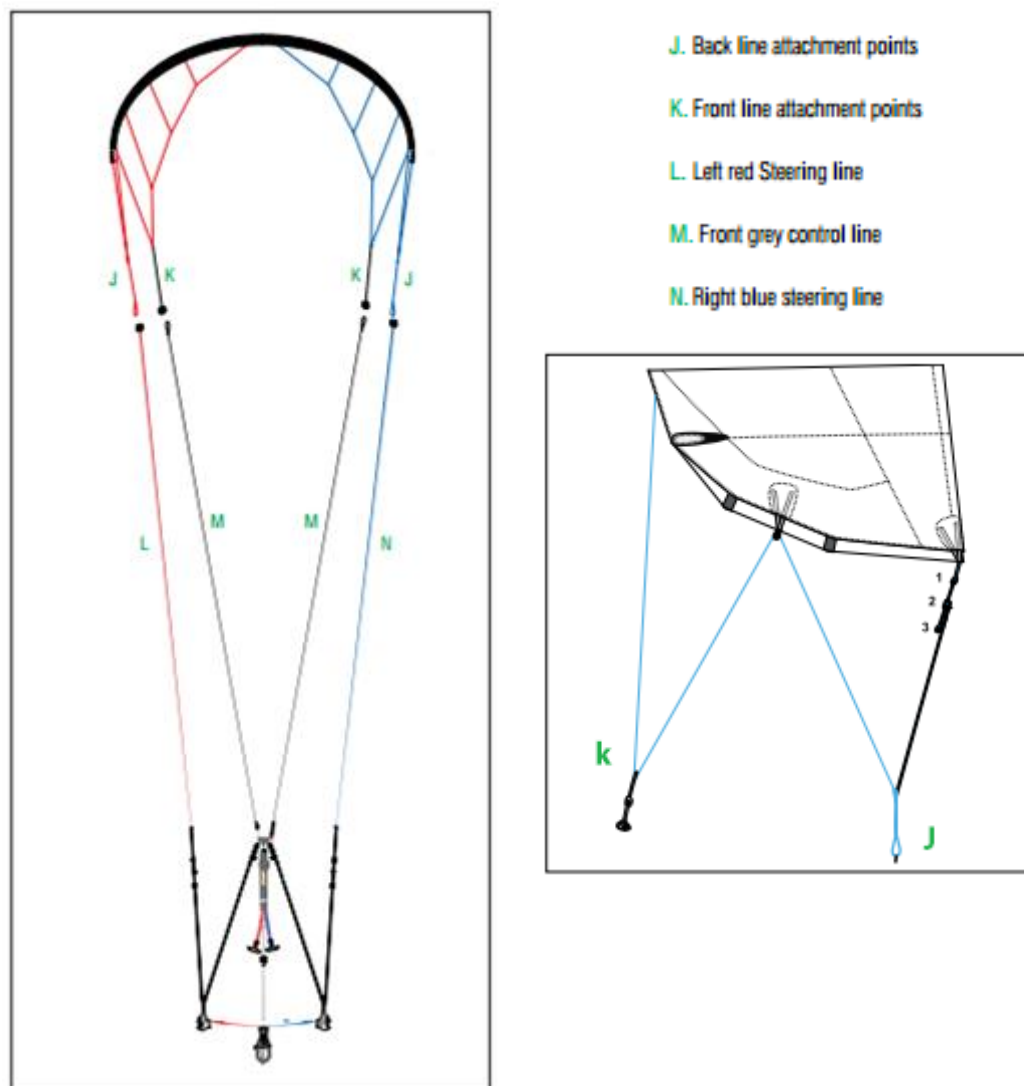


Figure 12. Kite lines scheme [18]

## 2.4 Effect of the angle of attack and the angle of inclination in kite power and kiter's balance.

The end of the explanation takes us to the last question: “Numerically, how is the power affected by the angle of attack and the inclination angle? And the overall equilibrium upon the kiter?”

There are four forces acting on the kite depending on their aerodynamic characteristics: lift on the Y-axis, drag and thrust on the Z-axis, and  $F_x$  on the X-axis. These forces are defined in the XYZ coordinate system. If the kite power is defined as the upward force pulling the kiter ( $T_y''$ ), both the power of the kite and the overall balance upon the kiter, are measured in the  $X''Y''Z''$  coordinate system. For this reason, a change from XYZ to  $X''Y''Z''$  coordinate system is necessary, and these changes are defined by the angle of attack and the inclination angle.

Figure 13 shows, at the top, the rotation of the XYZ coordinate system about the X-axis and, in the middle, how forces are defined accordingly to the  $X''Y''Z''$  coordinate system. Depending on the resultant force between drag and thrust, the orientation of the  $F_z'$  force will be positive or negative. This figure shows the case when  $F_z'$  is negative.

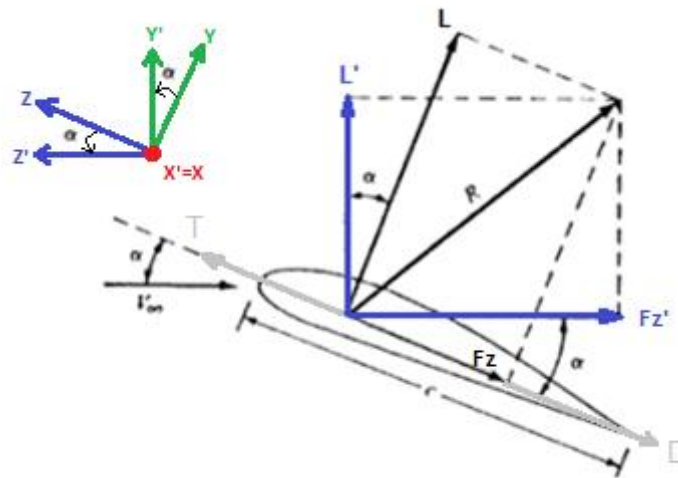


Figure 13. Vector forces decomposition.

In order to obtain the forces  $L'$  and  $F_z'$  from the  $X''Y''Z''$  coordinate system, the projections specified in equations 2.4.1 and 2.4.2. are used:

$$F_z' = L \sin \alpha - (T - D) \cos \alpha \quad (2.4.1)$$

$$L' = L \cos \alpha + (T - D) \sin \alpha \quad (2.4.2)$$

Now, to change from  $X'Y'Z'$  coordinate system to  $X''Y''Z''$  coordinate system there is a rotation about the  $Z'$ -axis as seen in figure 14. Besides, all the forces are supposed to be applied to the center of gravity of the kiter. Then, the forces in the  $X''Y''Z''$  coordinate system are the ones shown in the figure 14.

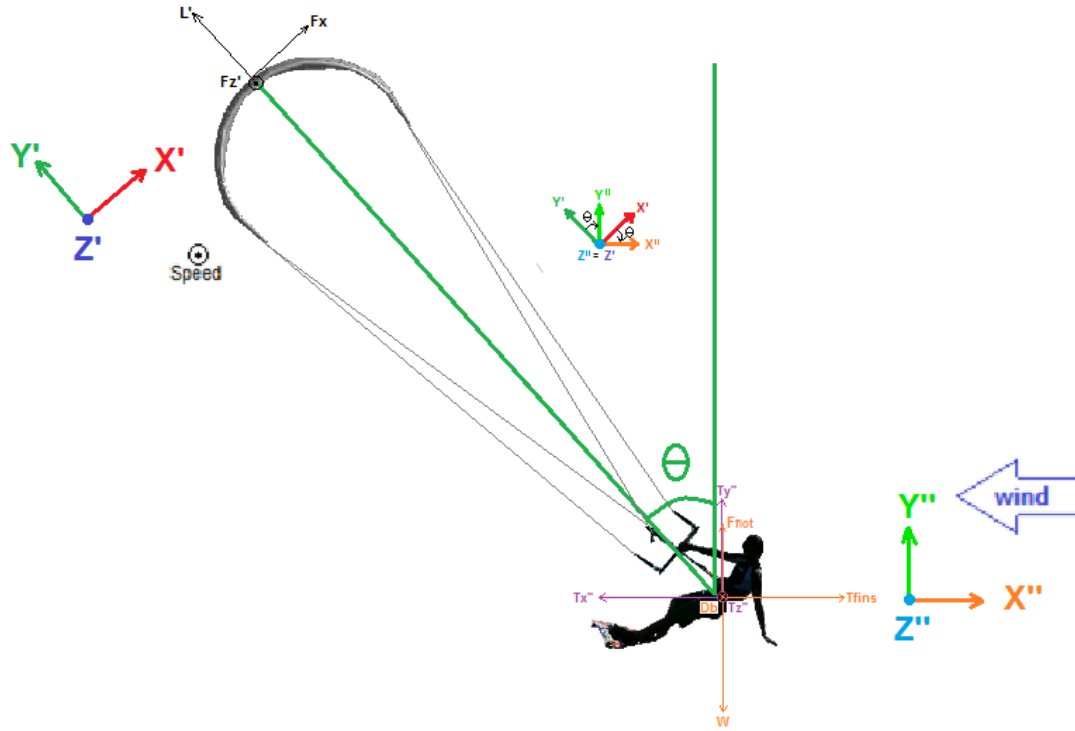


Figure 14. Forces scheme

The equations representing the figure 13 are the equations 2.4.3, 2.4.4 and 2.4.5.

$$T_x'' = F_x \cos\theta - L' \sin\theta \tag{2.4.3}$$

$$T_y'' = F_x \sin\theta + L' \cos\theta \tag{2.4.4}$$

$$T_z'' = F_z' \tag{2.4.5}$$

Besides, the following equations express the equilibrium of forces in the kiter. Remember that as said at the beginning of this chapter,  $F_{fins}$  is the force that opposes to  $T_x''$  using the board's fins and  $F_{flot}$  is the board's flotation force.

$$T_x'' = T_{fins} \tag{2.4.6}$$

$$T_y'' + F_{flot} = W = (m_{kiter} + m_{kite})g \tag{2.4.7}$$

$$T_z'' = D_b \tag{2.4.8}$$

If the equations 2.4.3, 2.4.4 and 2.4.5 are applied to the equations 2.4.6, 2.4.7 and 2.4.8, the equilibrium equations are the following ones:

$$F_x \cos \theta - (L \cos \alpha + (T - D) \sin \alpha) \sin \theta = T_{fins} \quad (2.4.9)$$

$$F_x \sin \theta + (L \cos \alpha + (T - D) \sin \alpha) \cos \theta + F_{flot} = (m_{kiter} + m_{kite})g \quad (2.4.10)$$

$$L \sin \alpha - (T - D) \cos \alpha = D_b \quad (2.4.11)$$

Let us now comment the summation equations. First of all, as said at the beginning of this chapter, all the forces applied to the kiter are concentrated in a point. Because of that, the change in momentums that kites use to sail is not taken into account. Consequently, the change on the lever-arm distance depending on the sail speed can't be studied. But for a kite aerodynamic study, it does not affect.

Another detail to remember is that in the aerodynamic study of the forces, a force called  $F_z$  appears, that it is the resultant force between drag and thrust. In all this study,  $F_z$  has been considered to be positive to simplify the equations. But in some cases,  $F_z$  can be negative as well.

Beside, as said in section 2.1 "Overview of the situation", the force given by the kite on the X''-axis ( $T_x''$ ) is equal to a force that here it was called  $T_{fins}$ . To maintain a trajectory perpendicular to the wind, the fins opposed to  $T_x''$ . In this work, this force cannot be simulated but its energy is supposed to dissipate into the water.

On the Y''-axis, it is considered that the board produces a significant flotation force. In this work, the only estimation done of this force is that it won't be as big as the one produced by a surf board. This is because there is already an upward force ( $T_y''$ ). This is why the manufacturers can make smaller boards that will cause less flotation force but will increase their manoeuvrability.

Finally, on the Z''-axis, only the kite's generated drag is computed and not the board's generated drag. The reason of this differentiation is that in this work only analyzes the aerodynamic behaviour of the kite and supposes that the drag of the board will be equal to  $T_z''$ , because this study has been done in a stationary situation.

## CHAPTER 3. SIMULATION APPROACH

The simulation consists of 5 phases: geometry, mesh, setup, solution and results. In each of the phases, the considerations that had been explained in the previous chapters will be applied and it will be seen the influence of them in the simulations. The last phase, results, is will be presented afterwards in the next section.

### 3.1 Geometry

In the first phase, the geometry, it was decided to fix the model and change the direction of the relative wind. As a result, all the simulations share the same geometry and mesh and only differ in the setup. This decision affected the shape of the domain as will be explained next.

When the model is fixed, the surface where the wind enters the domain has to be semisphere. For this reason, problems in vertices of the domain will be avoid when the wind direction change.

Besides, the two angles studied are  $\alpha$  and  $\theta$  which are comprised in orthogonal planes between them. The angle of attack is contained in YZ plane and the values are supposed to be from  $0^\circ$  to  $90^\circ$ . Though the usual interval of  $\alpha$  is unknown, the only limitation applied is what common sense says. Moreover, the inclination angle is contained in the XY plane and the range of values is the same that the angle of attack. Then, the x and z components of the wind will always be negative and the y component always positive. Because of this, the main domain is divided in two parts. The upper part with the furthest surface is the outflow and the lower part is the inflow.

Figure 15 shows the geometry used and all the important characteristics. Wind and relative wind are decomposed using the angle of attack and inclination angle.

Furthermore, figure 15 shows the semisphere and the division of upper part and lower part of the domain too.

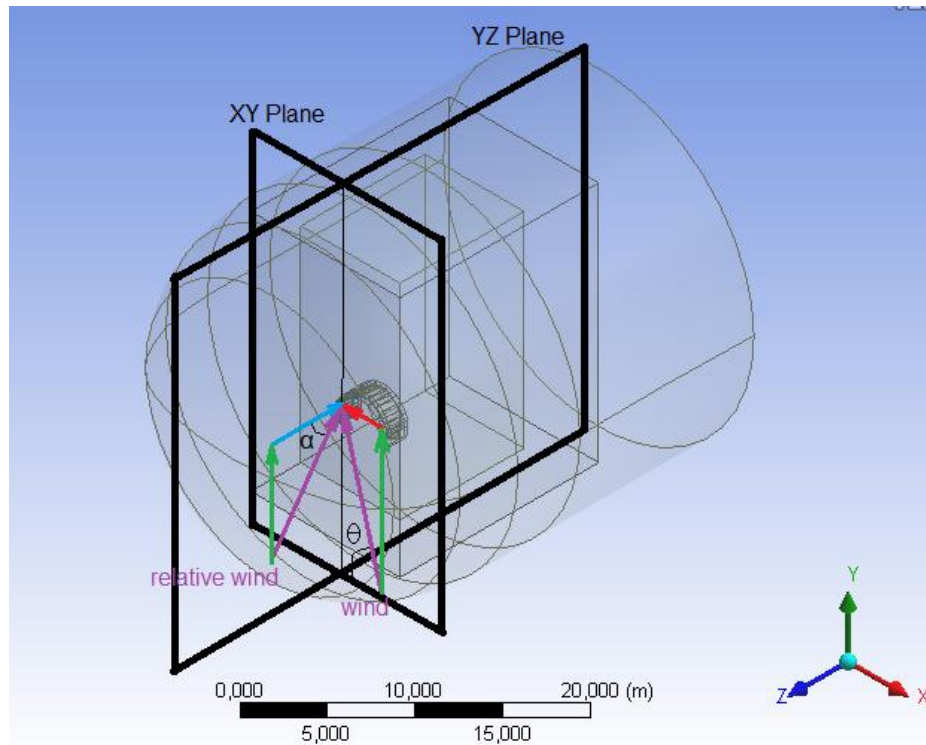


Figure 15. Geometry

### 3.2 Mesh

Mesh is the second phase. Once the geometry is finished, the computer resources are optimized trying to find values of sizing and inflation to have enough accuracy in the results. As seen in figure 15, there are three sizing boxes to determine the optimum value in each zone, and a good transition of element sizes between them. The final number of elements to have a good approximation is 1494710 elements. Figure 16 shows a section of the domain meshed.

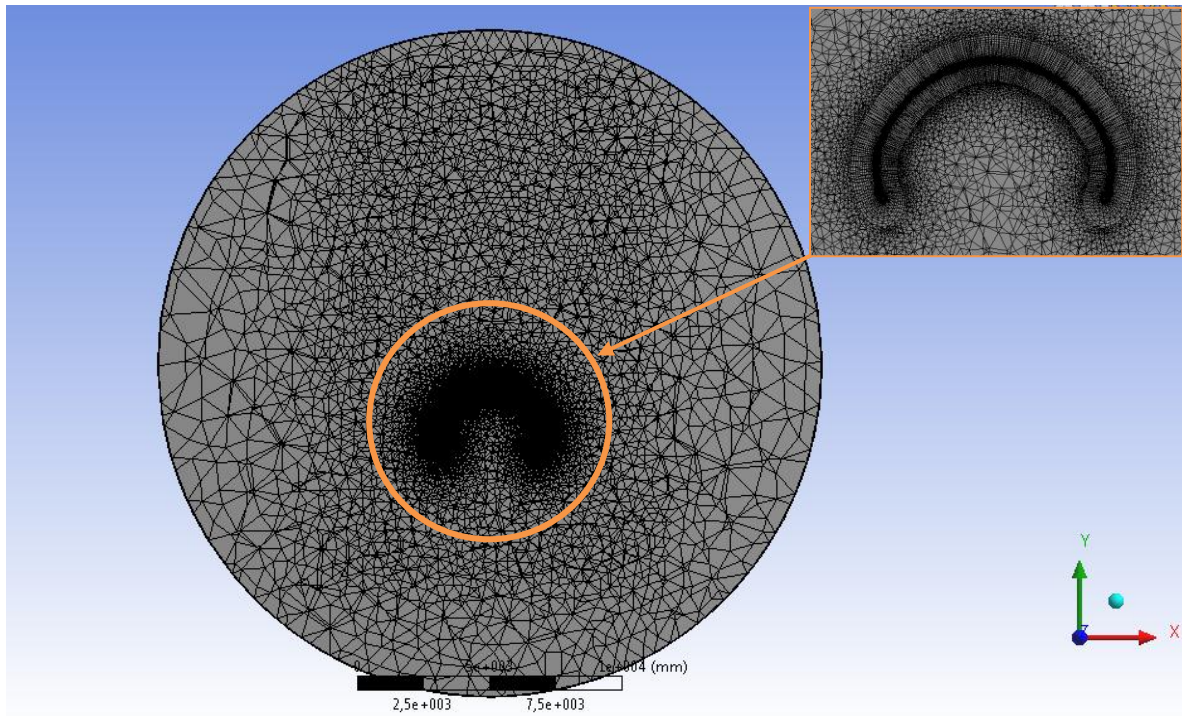


Figure 16. Section of the domain

### 3.3 Setup

In the setup, the inlet and outlet surfaces are defined as said in the geometry. But there is an exception when the angle of attack is low. If these cases are not treated different, the velocity would be not uniform where the domain is not affected by the kite. Figure 17 shows the different inlet surface definition for low angles of attack in the left image, and the general definition in the right image.

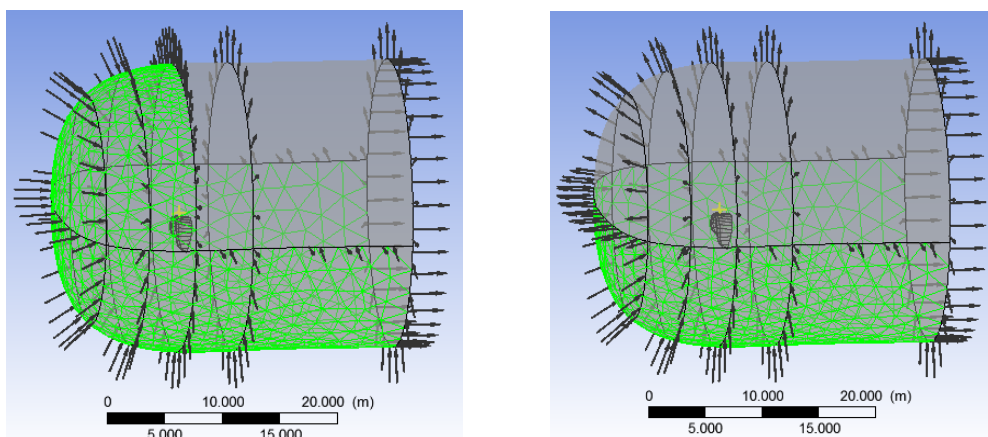


Figure 17. Definition of the inlet surface (left image is for a low  $\alpha$  and right for a high one).

The inlet input is specified in the Cartesian components of the wind and the outlet with the absolute pressure. However, the kite's surfaces are defined as wall no-slip due to the foil's low coefficient of friction. The fluid is air at 25°C and at medium turbulence, 5%. The last input is the initialization with the inlet wind to ease the computation and the turbulence model.

There are two series of results that differ from the intensity of wind speed. Remember that the wind range for this kite model is between 7 m/s and 17 m/s. Although the kite speed and the wind speed are supposed to have a relation of 1.5 times, that is a true representation of reality only in case of the best kite's performance. That can depend on many factors that cannot be computed. Both wind speeds are supposed to produce the best kite's performance, and this is the reason why two close wind speeds are chosen. Doing so, variations in the aerodynamic behaviour can be seen without the influence of this ratio change. The first series is computed with wind speed equal to 10 m/s and the second with 12 m/s.

Finally, the initialization is different between the series. The 10 m/s series converges well. But in the 12 m/s series, the turbulence increases a lot. To get good results without changing the common inputs with the first series, the turbulence model in the initialization and solver was the key. So, finally, the turbulence model used in the first series is Medium Intensity and Eddy Viscosity Ratio and the second series is High Intensity and Eddy Viscosity Ratio. Meanwhile, in the solver the turbulence model is of First order and in the second is High resolution.

### 3.4 Solution

The last phase explained in this section is the solution. The CFD solver used is CFX that computes each case until the convergence. Generally, the solver will consider that it converges when the momentum and mass residues is under  $1e-5$ , and the velocity in the zenith of the kite, in the Cartesian coordinates (0,3,-0.5), is constant. But, in some special cases, because of the turbulence in the domain, the residues couldn't be less than  $1e-4$ . However, it is considered a good approximation to the result if the velocity in the zenith of the kite is constant.

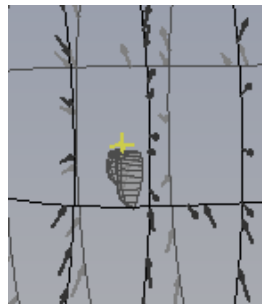


Figure 18. Zenith point of the kite, where the velocity is evaluated.

Figure 19 shows the case when a  $1e-5$  momentum and mass residues is achieved. As it can be seen in figure 20, the turbulence, in this case, decreases considerably when the velocity shown in figure 21 is constant. But not in all the situations, a low level of turbulence is achieved.

Besides, there are two series with different wind speeds. But each series has combinations of 4 different angles of attack and 5 different inclination angles. There is not any study about which values of angles are interesting in a kite. This is why; the values taken are useful for a first glance of which of them are more characteristic of the kite performance. The values chosen for  $\alpha$  are:  $30^\circ$ ,  $45^\circ$ ,  $60^\circ$  and  $80^\circ$ . Meanwhile, the values for  $\theta$  are:  $0^\circ$ ,  $30^\circ$ ,  $50^\circ$ ,  $70^\circ$  and  $90^\circ$ . Though the extreme values of  $\alpha$  are impossible to be used in a real situation, they can give some extra information.

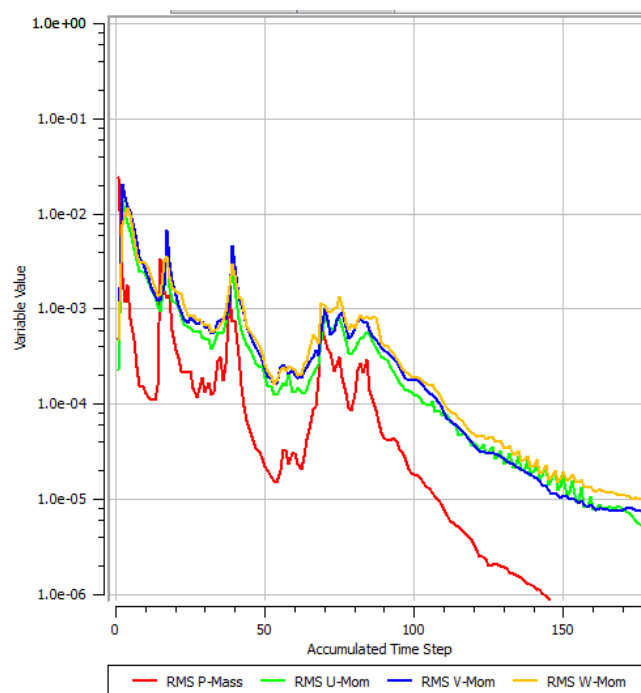


Figure 19. Momentum and massa residues ( $\alpha=30^\circ$ ,  $\theta=50^\circ$ , wind speed =12 m/s )

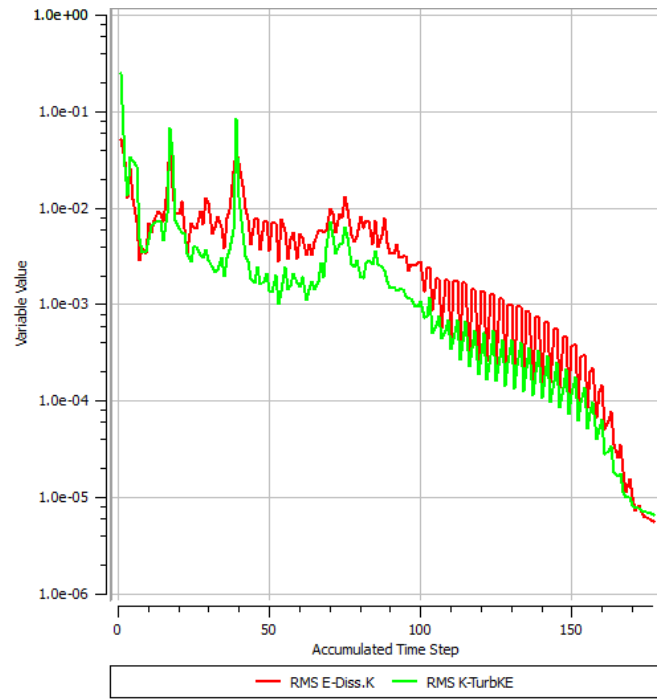


Figure 20. Turbulence residues ( $\alpha=30^\circ$ ,  $\theta=50^\circ$ , wind speed =12 m/s )

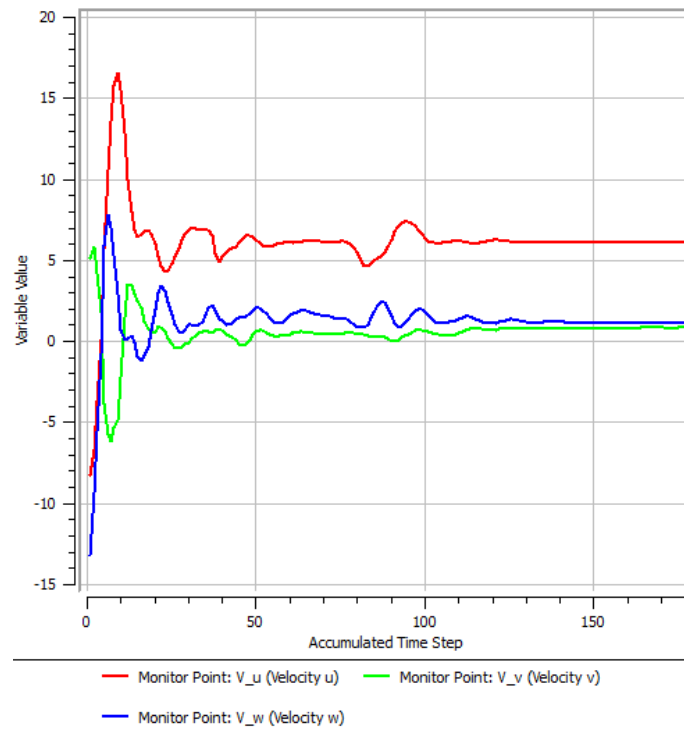


Figure 21. User's point residues ( $\alpha=30^\circ$ ,  $\theta=50^\circ$ , wind speed =12 m/s )

## CHAPTER 4. RESULTS

In this chapter, first the data available of the simulations is presented. Then, the aerodynamic forces generated on the kite are analysed depending on the three variables that were explained before and, after, how this forces act upon the kiter. An important part of the last section is justified in which cases the kite can be in a stationary situation and when not.

### 4.1 Data obtained

There are two types of data that can be useful in this work: pressure and velocity countours and expressions of the forces in each axis. The countours show how a variable value in the entire domain and they use a colour scale. The expressions are equations that calculate the value of a variable or a coefficient for a specific region.

Figure 22 is a velocity contour for the same case as figures 19, 20 and 21. This figure is in the kite's symmetric plane. Meanwhile, figure 23 is the pressure contour with the same section and case as figure 22. Both figures show the same behaviour because both are the cause of the forces generated that will be analysed afterwards.

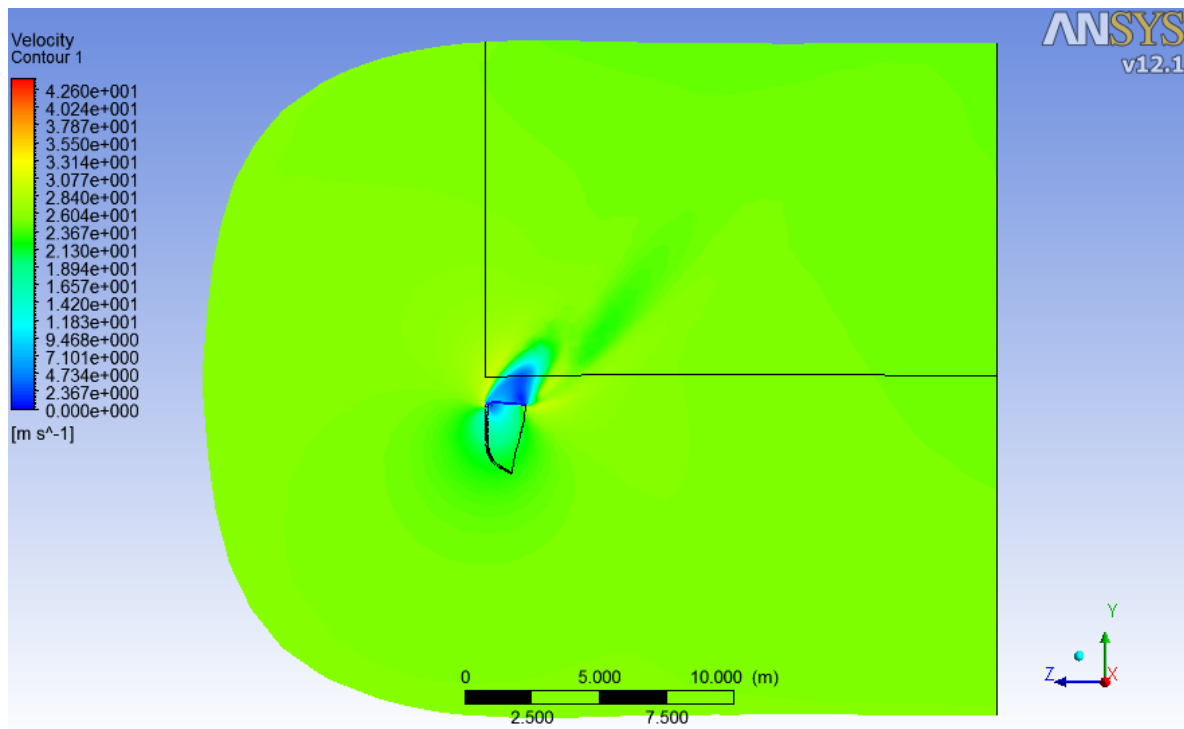


Figure 22. Velocity contour ( $\alpha=30^\circ$ ,  $\theta=50^\circ$ , wind speed =12 m/s )

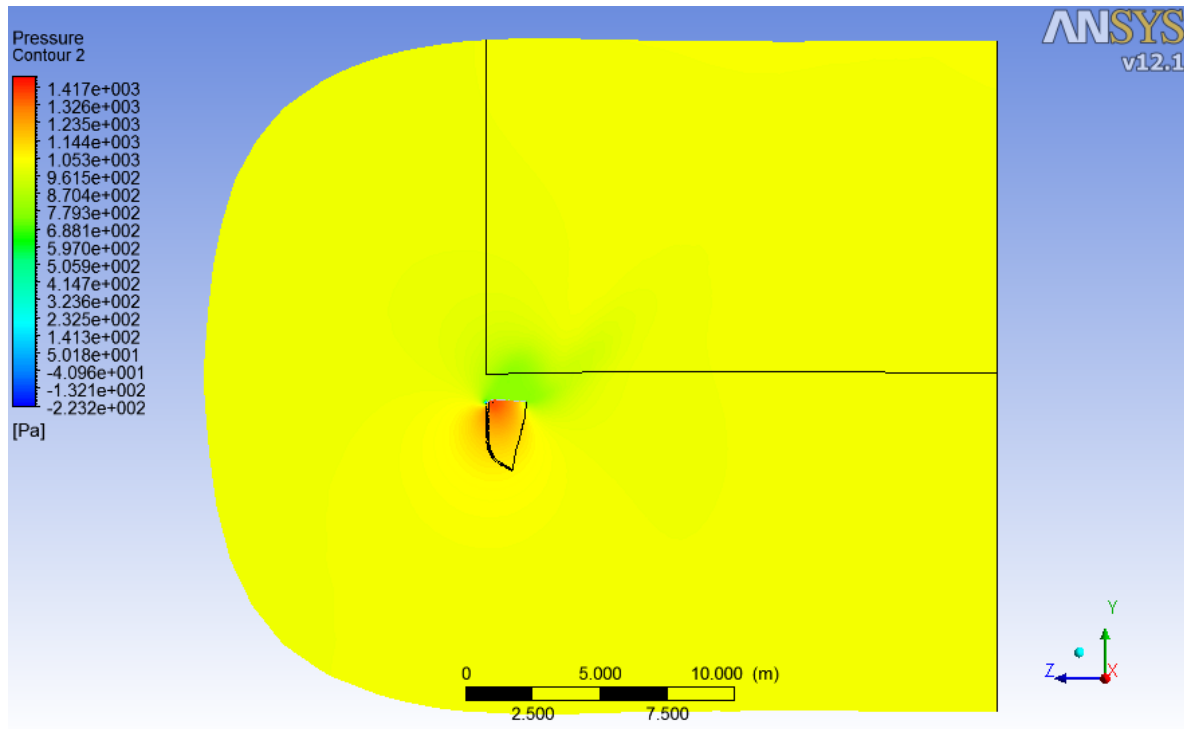


Figure 23. Pressure contour ( $\alpha=30^\circ$ ,  $\theta=50^\circ$ , wind speed =12 m/s )

Moreover, the expressions used in the following analysis are the forces in each axis: lift,  $F_x$  and  $F_z$ . All these equations are alike. For example, the lift expression is shown in figure 24.

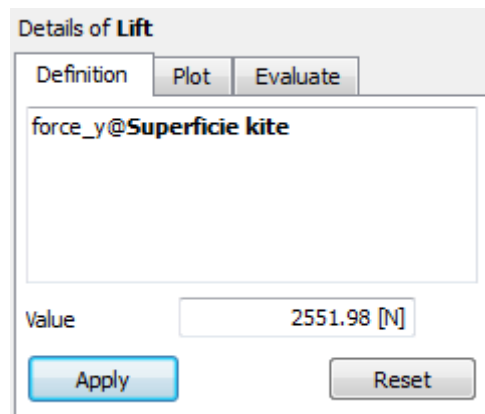


Figure 24. Lift expression ( $\alpha=30^\circ$ ,  $\theta=50^\circ$ , wind speed =12 m/s )

## 4.2 Aerodynamic behaviour analysis

There are 3 resultant forces acting on the kite due to their aerodynamic characteristics: lift,  $F_z$  and  $F_x$ . Here, the change of these forces will be studied

depending on three variables: wind speed, the angle of attack  $\alpha$  and the inclination angle  $\theta$ .

In the following charts the direction, orientation and module of these forces can be observed depending on these variables.

#### 4.2.1 Lift

Lift is the resultant force in Y-axis produced by the difference of pressure between the upper and lower surface of the kite's foil along the entire arc. This effect was shown in figure 23. Remember as commented on the first chapter, that a kite flatter produced more lift. That happens because if there is more surface that produce this difference of pressure in the direction of Y-axis, more lift will be created.

Figure 25 shows when the wind speed is 10 m/s and how lift changes depending on the angle of attack and the inclination angle. Meanwhile, figure 26 is when wind speed equal to 12 m/s.

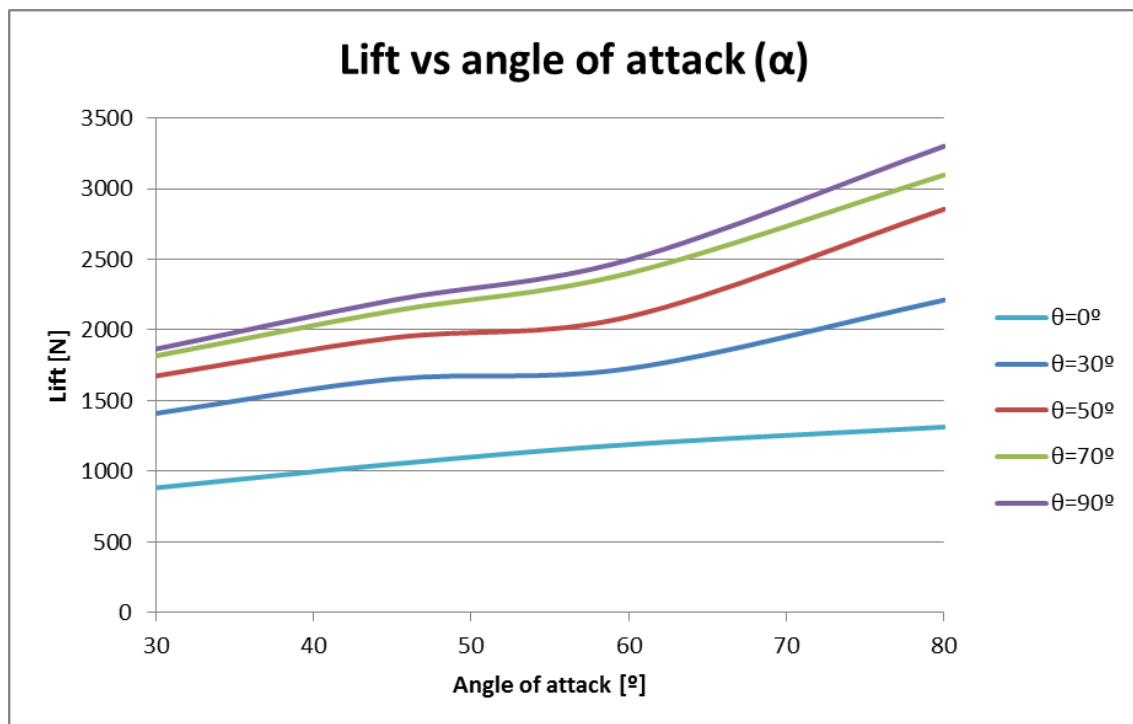


Figure 25. Lift depending on  $\alpha$  for different  $\theta$  (wind speed = 10 m/s).

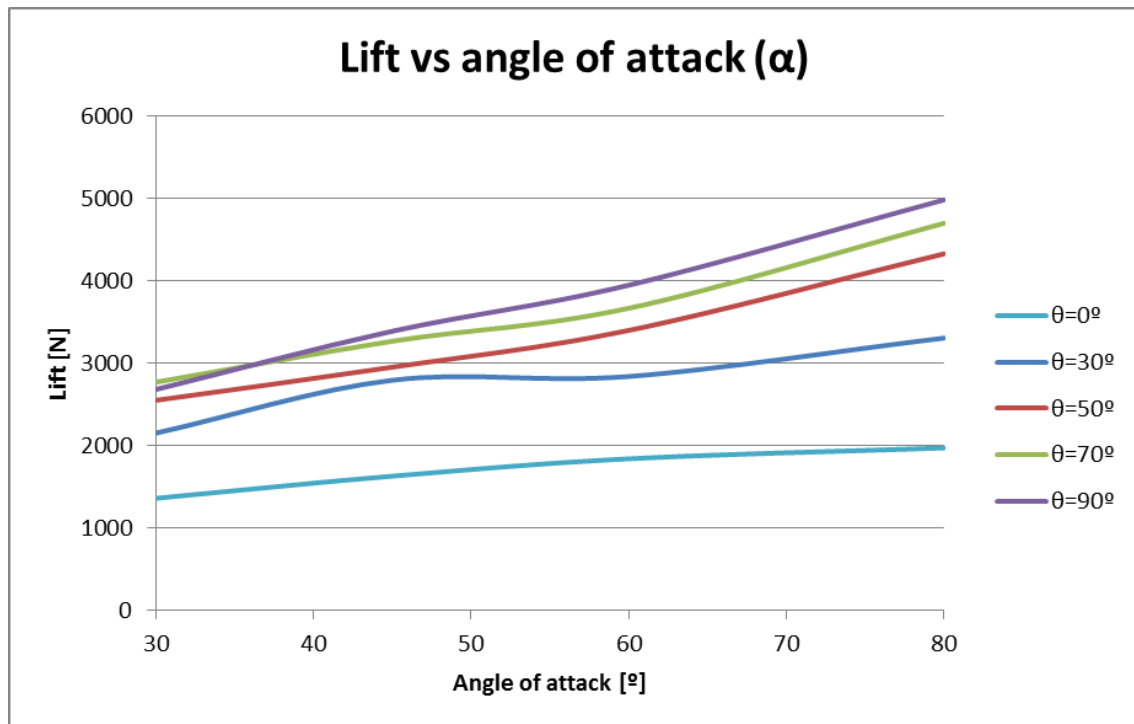


Figure 26. Lift depending on  $\alpha$  for different  $\theta$  (wind speed = 12m /s).

The general tendency is to grow significantly when  $\alpha$  rises, as in a common airfoil. Besides, for the same  $\alpha$ , as the  $\theta$  increases, the lift goes up. When  $\alpha$  is 30°, in figure 25, the values are between 900N and 1900 N. But in figure 26 the values grow to be between 1400 N and 2700 N. Furthermore, when  $\alpha$  is equal to 80° in figure 25 are between 1800 N and 3300 N. In figure 26, the values are between 1900 N and 5000 N. This result confirms the knowledge of kites that is usually expressed with figure 27, the wind window.

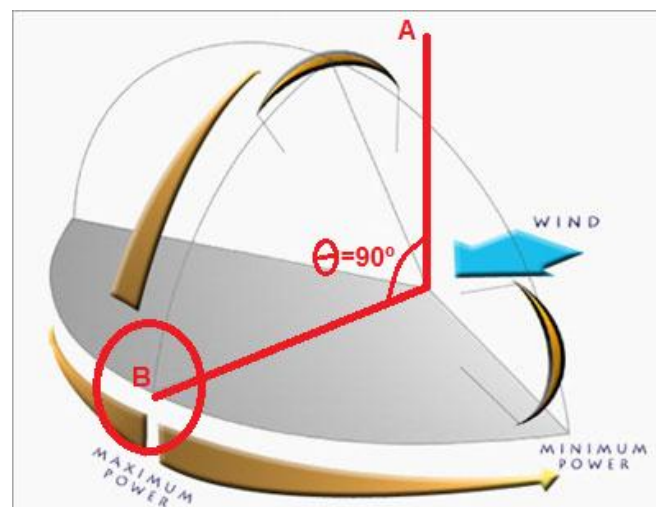


Figure 27. Wind window

In a stationary situation, the position in the wind window is between the point A and B, where A will correspond to  $\theta=0^\circ$  and B to  $\theta=90^\circ$ . As confirmed in the figure 28, when the difference of pressure between the upper and lower surface increases, lift is bigger and the other way around.

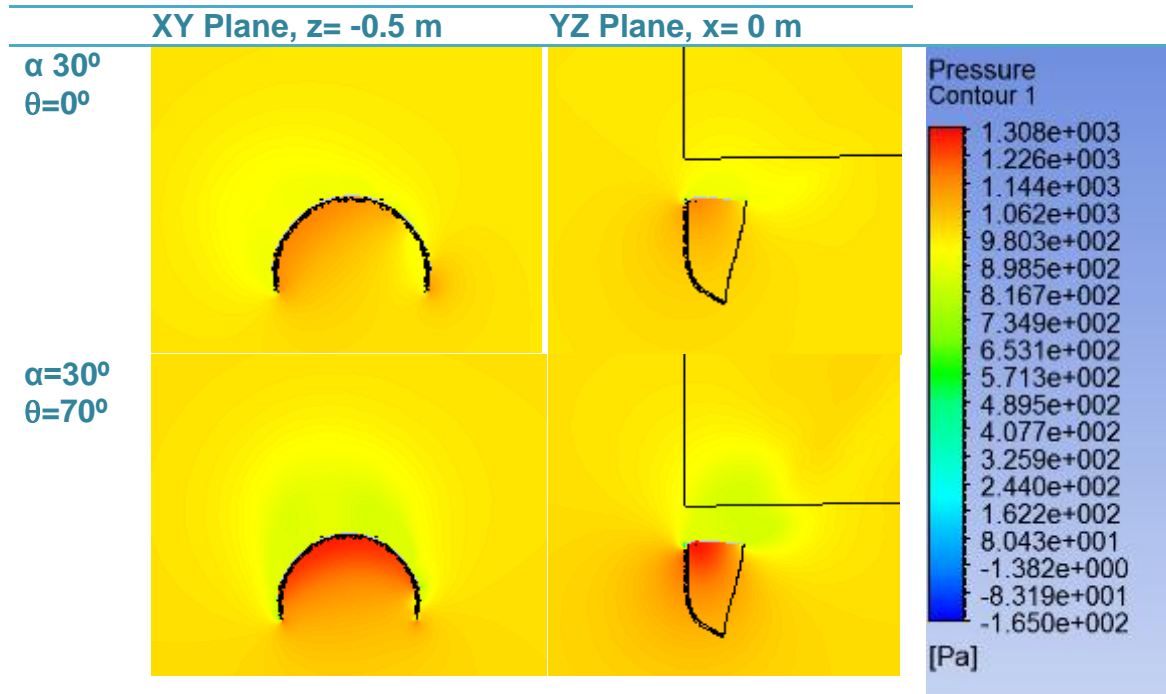


Figure 28. Table of Fx comparison depending on  $\theta$

The explanation is really easy. With the same intensity of wind and kite speed, when the inclination angle increases, the component in the Y-axis of the resultant velocity is bigger than the component in X-axis. The following equations confirm that:

$$v_x = -v_{wind} * \cos \theta \quad (4.2.1.1)$$

$$v_y = v_{kite} * \sin \alpha + v_{wind} * \sin \theta \quad (4.2.1.2)$$

$$v_z = -v_{kite} * \cos \alpha \quad (4.2.1.3)$$

#### 4.2.2 Fx

This force is the resultant force in X-axis produced by the difference of pressure between the upper and lower surface of the kite's foil along the entire arc. In an airplane airfoil, this force is inexistent due to the fact that the wind is perpendicular to the resultant force produced by this difference of pressure. In that case, lift and Fx are the decomposition in XYZ coordinate system of the same force acting on any airplane's airfoil.

Figure 29 shows the pressure around the kite in a XY Plane, near the leading edge when the wind speed is 10 m/s,  $\alpha$  is  $60^\circ$  and  $\theta$  is  $30^\circ$ . As shown before, the difference of pressure is not totally parallel to the Y-axis.

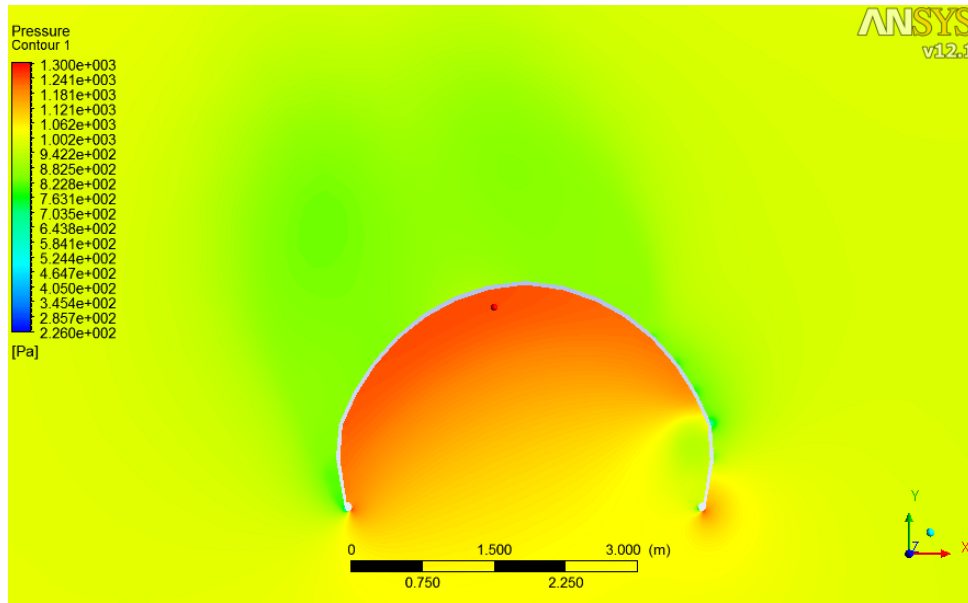


Figure 29. Pressure distribution around the kite ( $\alpha$  is  $60^\circ$ ,  $\theta$  is  $30^\circ$  and wind speed is 10 m/s)

Figure 30 and 31 shows the  $F_x$  depending on  $\alpha$  and  $\theta$  in case of wind speed 10 m/s and 12 m/s, respectively.

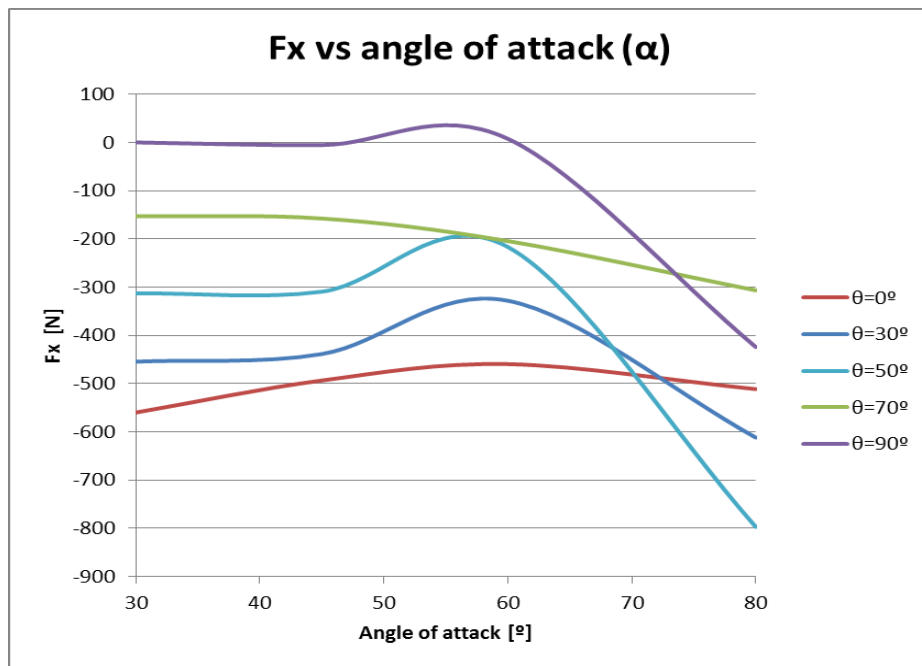


Figure 30.  $F_x$  depending on  $\alpha$  and  $\theta$  (wind speed = 10 m/s)

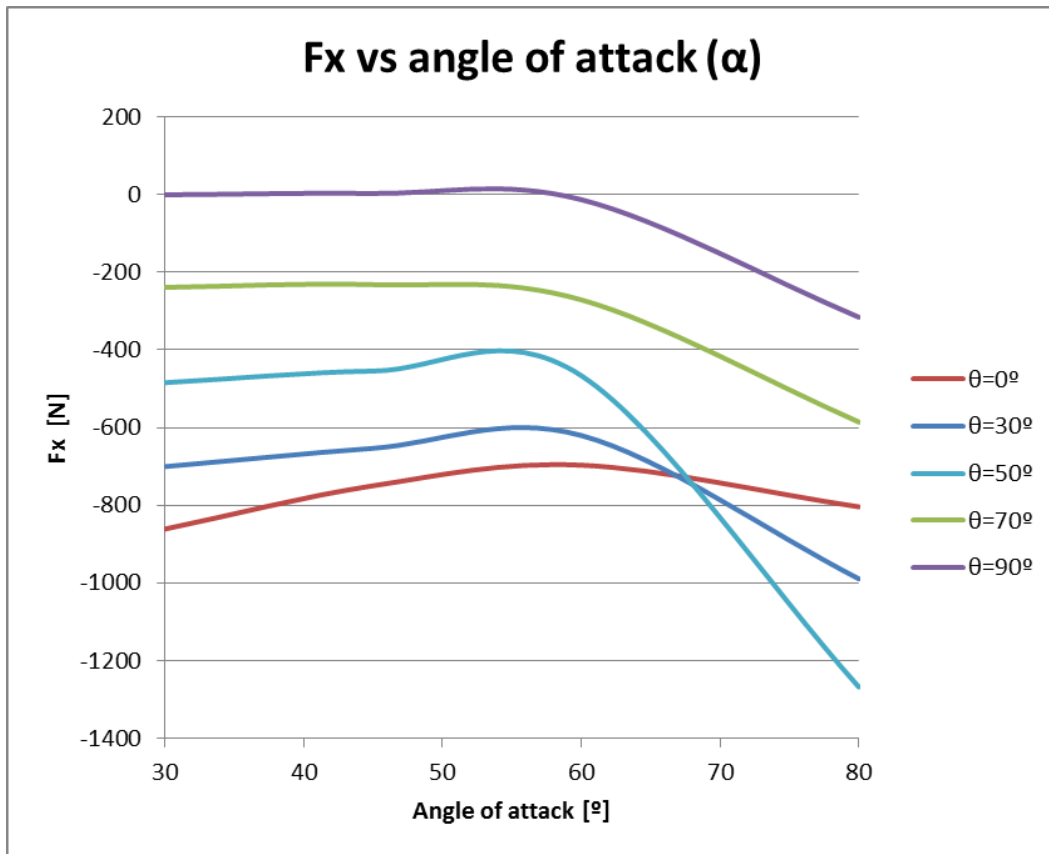


Figure 31.  $F_x$  depending on  $\alpha$  and  $\theta$  (wind speed = 12 m/s)

Both graphs are really similar. Only the extreme values are a little different.  $F_z$  is always negative, but when  $\alpha$  is  $60^\circ$ , almost in all configurations, a significant increase, in absolute value, of  $F_x$  is produced. After it will be explained which are the possible configurations. But only say, that a change of trend when  $\alpha$  is equal to  $60^\circ$  is not an important feature to study. Consequently,  $F_x$  remains almost steady in some cases or with a low slope with  $\alpha$  increases.

On the contrary, the reason why there is a considerably difference depending on the value of  $\theta$  is an interesting question. The same equations to explain the behaviour of the lift depending on  $\theta$  justifies the behaviour of  $F_x$ . When the difference of pressure between the upper and lower surface is small,  $F_x$  is bigger, because the component of velocity in the X-Axis increases when the difference decreases.

#### 4.2.3 Lift i $F_x$

Both forces are generated due to the difference of pressure between the upper and the lower surface of the kite. Therefore, the lift generated on a common airfoil is comparable to the vectorial sum of lift and  $F_x$ . Let us see the contribution of this resultant force ( $F_p$ ). Figures 32 and 33 show the module of

$F_p$  and figures 34 and 35 show the difference of  $F_p$  in module and angle with respect to the lift that is produced by  $F_x$ .

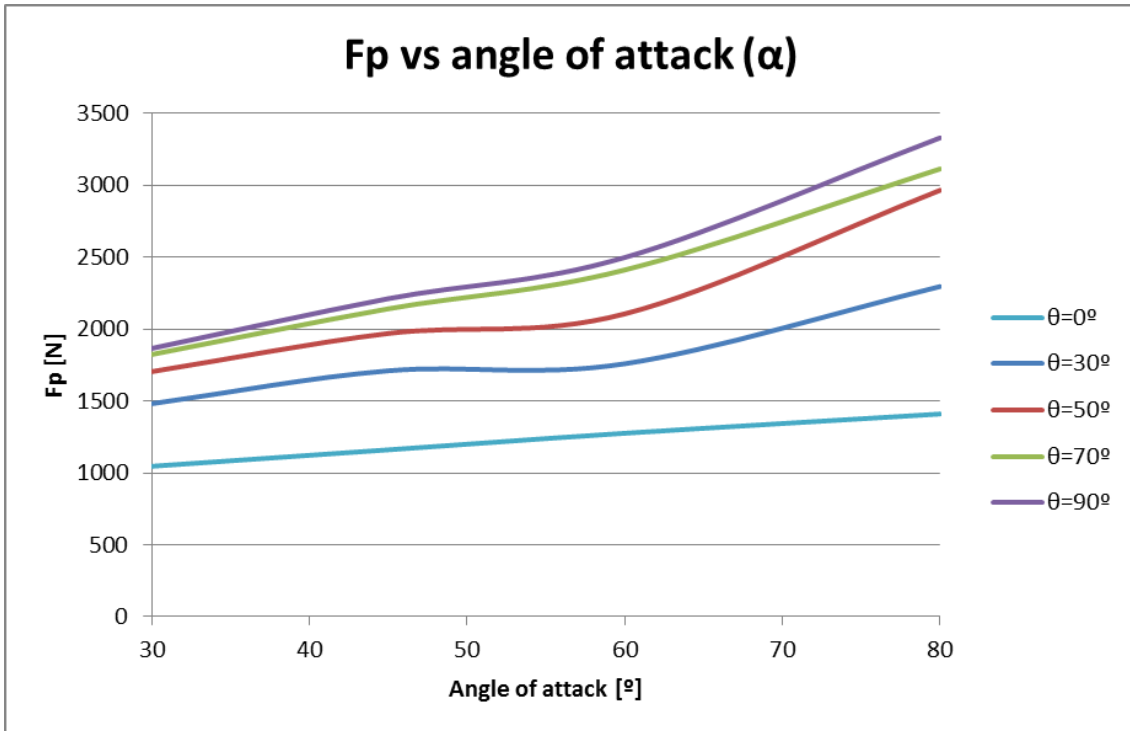


Figure 32. Resultant force ( $F_p$ ) of lift and  $F_x$  (wind speed= 10 m/s).

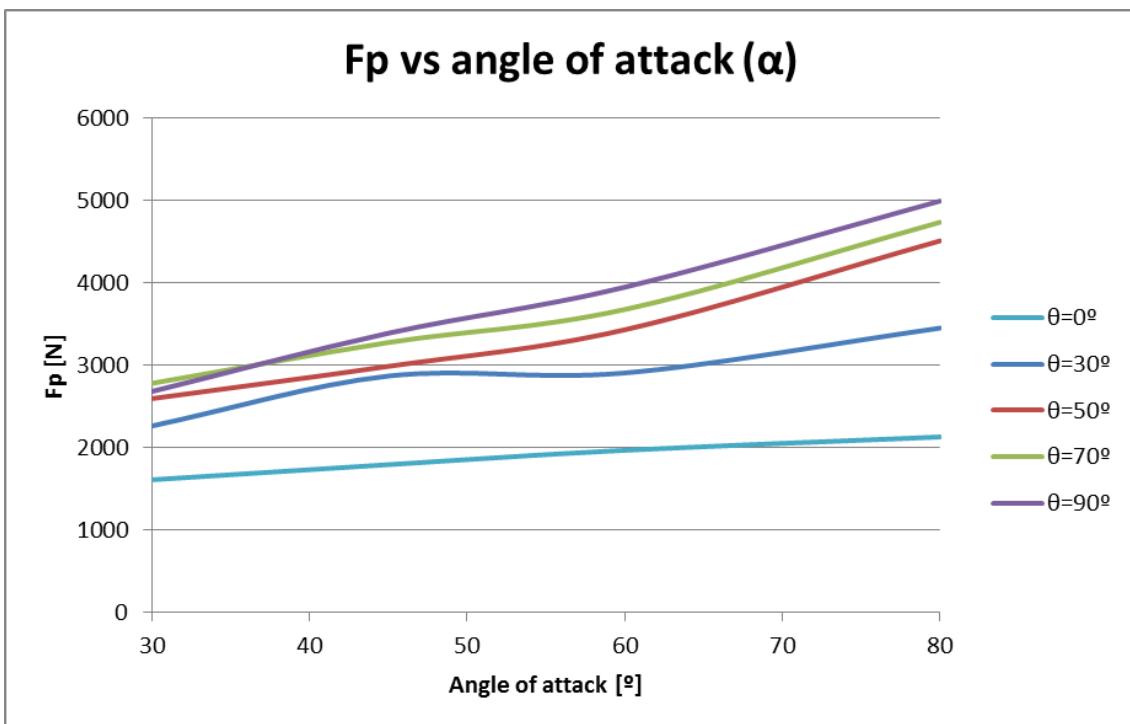


Figure 33. Resultant force ( $F_p$ ) of lift and  $F_x$  (wind speed=12 m/s).

$\theta$	wind	$\alpha=30^\circ$	$\alpha=45^\circ$	$\alpha=60^\circ$	$\alpha=80^\circ$
$0^\circ$	10 m/s	162.58663	110.20541	85.740346	96.088962
	12 m/s	249.199011	163.954106	127.338238	157.410203
$30^\circ$	10 m/s	71.470135	57.264916	30.899187	83.086293
	12 m/s	111.013446	75.2965319	66.9139084	144.843456
$50^\circ$	10 m/s	28.97811	24.475256	11.186636	109.23658
	12 m/s	45.5074737	34.7291841	31.8242667	181.978807
$70^\circ$	10 m/s	6.4140532	5.8171464	8.696359	15.139908
	12 m/s	10.2643435	8.20765007	9.98164626	36.3390756
$90^\circ$	10 m/s	1.79E-07	0.0067981	0.01153	27.159227
	12 m/s	2.3637E-05	0.00152199	0.02057756	9.99206376

Figure 34. Table comparing the module of  $F_p$  with respect to lift.

$\theta$	wind	$\alpha=30^\circ$	$\alpha=45^\circ$	$\alpha=60^\circ$	$\alpha=80^\circ$
$0^\circ$	10 m/s	0.5650063	0.4392457	0.3687445	0.3713463
	12 m/s	0.56338512	0.43058703	0.36155348	0.38669768
$30^\circ$	10 m/s	0.3118889	0.2595278	0.1877335	0.2698734
	12 m/s	0.31436499	0.22953145	0.2149107	0.29066624
$50^\circ$	10 m/s	0.1846795	0.1578203	0.1031234	0.2723154
	12 m/s	0.18746308	0.15259786	0.1362763	0.28498638
$70^\circ$	10 m/s	0.0838966	0.0737307	0.0849635	0.0986619
	12 m/s	0.08591638	0.07078403	0.07367845	0.12393642
$90^\circ$	10 m/s	1.385E-05	0.0024795	-0.0030388	0.1278265
	12 m/s	0.00013272	-0.00094743	0.00322803	0.06326566

Figure 35. Table comparing the angle of  $F_p$  with respect to the lift

As seen in figure 32 and 33, the trend of the  $F_p$  is the same as the lift have and this is confirmed by the tables of figure 34 and 35. The maximum change in module is around 249 N, but is the case when less lift is generated,  $\alpha=30^\circ$  and  $\theta=0^\circ$ . When  $\alpha$  or  $\theta$  increases, this difference decreases roughly.

To sum up, although the wind  $X''$ , perpendicular to the kite speed (speed  $Z''$ ), can cause a variation in the direction of the force, produced by the difference of pressure ( $F_p$ ), the main component of  $F_p$  is the one parallel to Y-Axis.

#### 4.2.4 $F_z$

$F_z$  is the resultant force between the thrust and the drag. In an airplane airfoil, there is drag but not thrust generated. For that reason, the kite produces a positive force in the Z-axis that could be for different factors. It might be because of the different configuration of the winds or the effect of the curvature of the kite. The possible reason that seems more logical is the first, the different configuration of the winds. As a ship does, they use the wind to inflate the sail

and obtain thrust. The curvature of the kite could be to get profit of the maximum of area exposed to the wind in all the range of  $\theta$ . In figure 36 and 37 there are the values that take these forces depending on our variables.

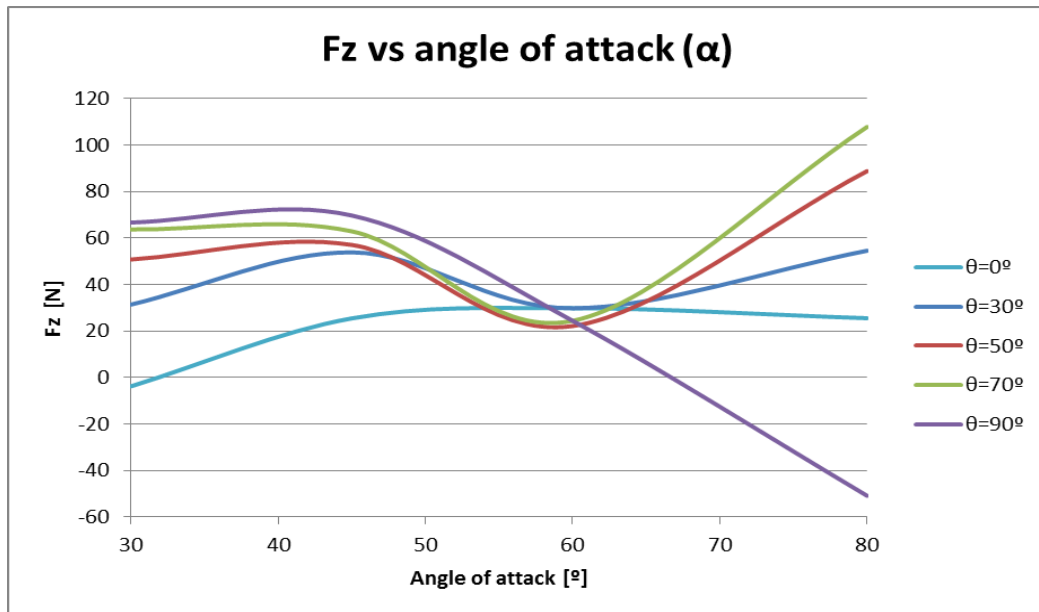


Figure 36. Fz depending on  $\alpha$  and  $\theta$  (wind speed = 10 m/s)

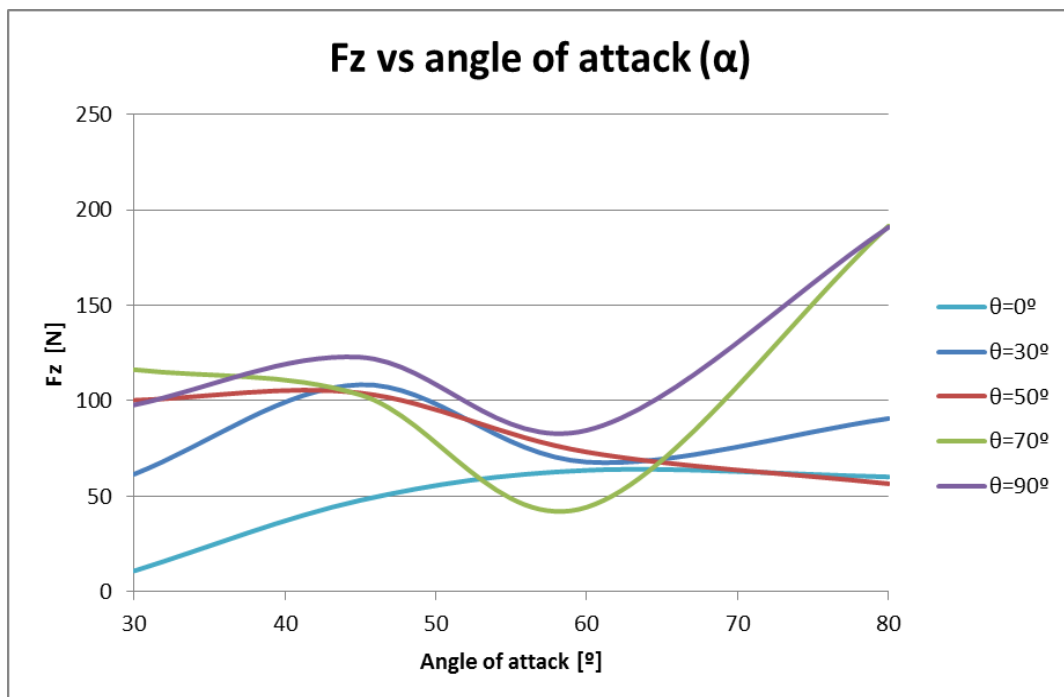
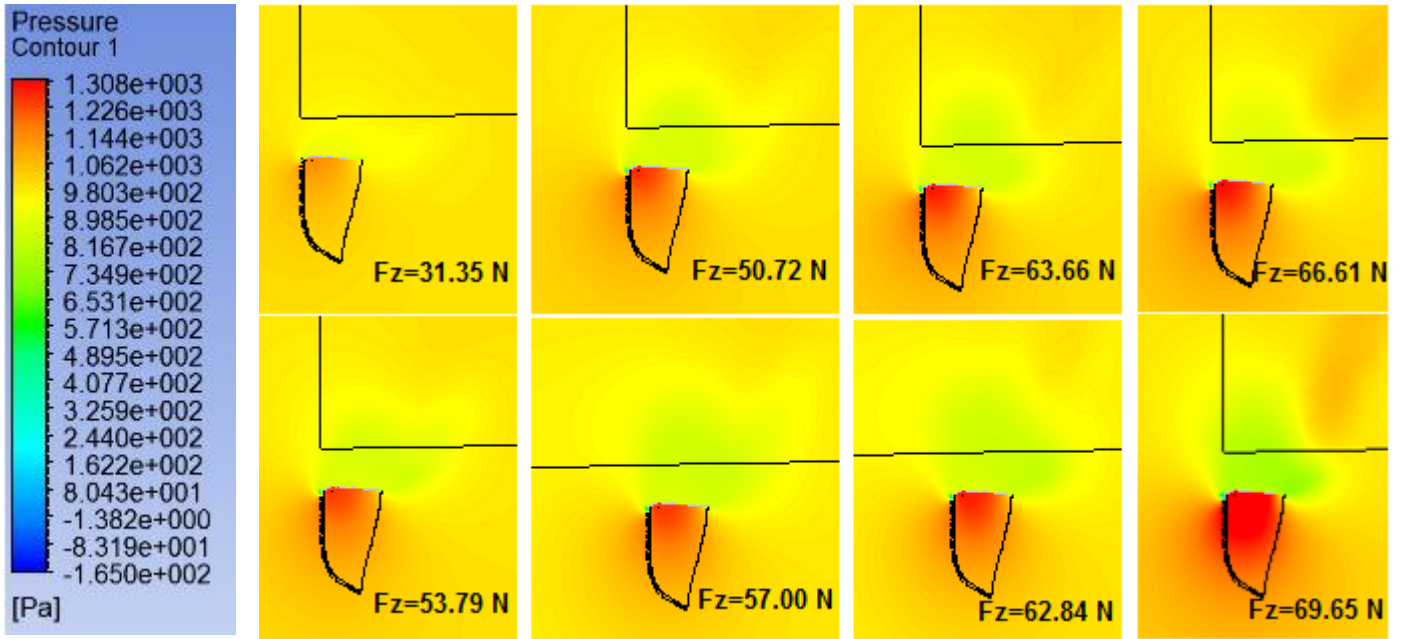


Figure 37. Fz depending on  $\alpha$  and  $\theta$  (wind speed = 12 m/s)

The  $F_z$  graphs change roughly in both cases. In  $45^\circ$  there is a peak, whereas in  $60^\circ$  there is a quickly drop. This could have meant that until  $45^\circ$ , the drag doesn't affect so much but after the  $45^\circ$  peak, the drag rocket.

There is of not much importance for the configurations with  $\alpha$  bigger than  $45^\circ$ , this will be explained after in more detail.

To justify the change in  $F_z$  depending on  $\alpha$  and  $\theta$ , figure 38 is really useful to know the pressure pattern.



**Figure 38. Pressure contour of the YZ Plane,  $x=0$  m ( figures in the first row have  $\alpha=30^\circ$  and the second row  $\alpha=45^\circ$ , starting from the left theta increases from  $0^\circ$  to  $90^\circ$ )**

As seen in Figure 38, when the difference of pressure increases, when  $\alpha$  or  $\theta$  increases, an increase in  $F_z$  is seen. When velocity contours of the extreme values are seen, as in figure 39, they show a common behaviour, as it would be expected. The additional information that they provide is the wake that the kite leaves behind. For this reason, the behaviour of  $F_z$  is justified taking into account that the wake does not seem turbulent yet and the component of drag has a still relative low value.

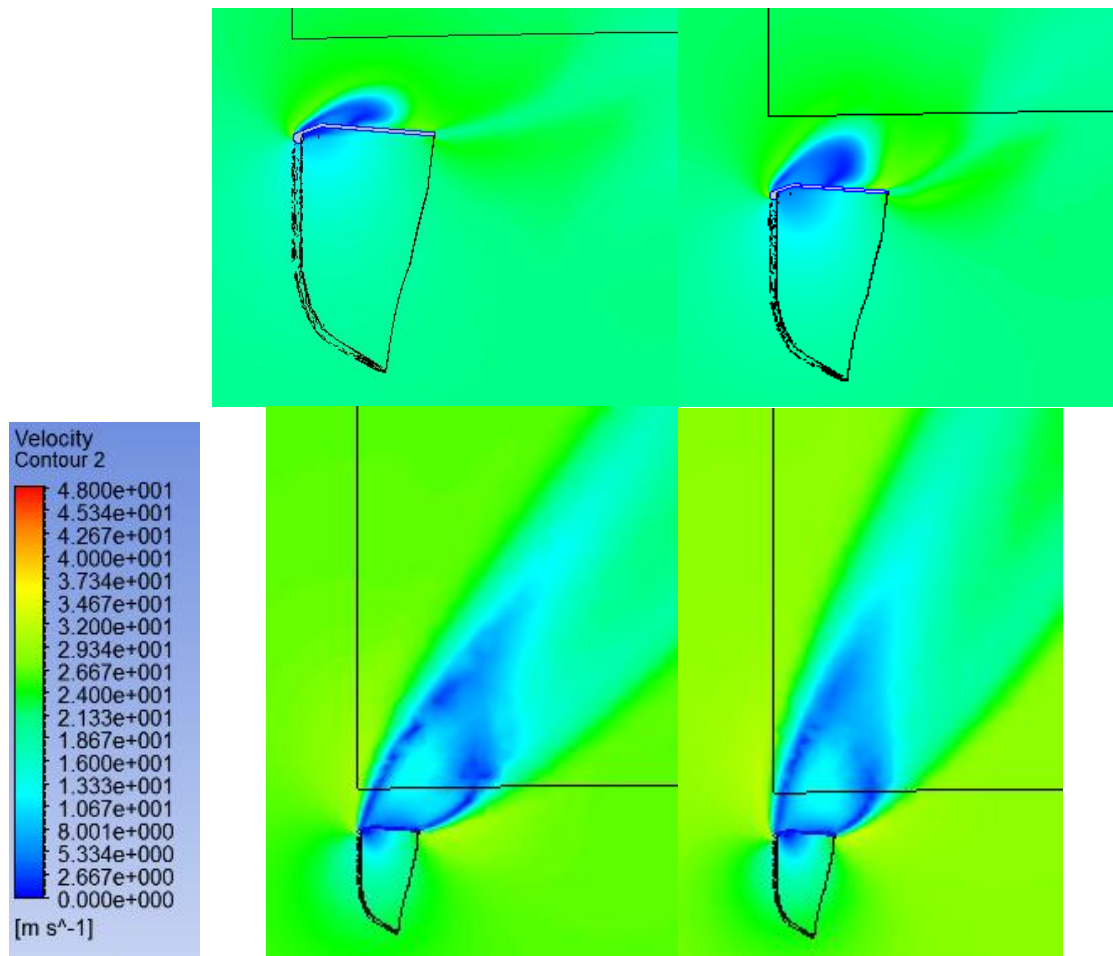


Figure 39. Velocity contours of the YZ Plane, x=0 m (figure in the first row have theta=0° and in the second row theta=90°, the first column alpha=30° and the second alpha=45°).

### 4.3 Analysis of the forces applied to the kiter

The forces acting upon the kiter have been decomposed in the X'', Y'' and Z''-axis. These forces are called Tx'', Ty'' and Tz'' because the forces are transmitted by the kite lines.

In the following charts, the direction, orientation and module of all these forces can be seen depending on these three variables.

#### 4.3.1 Force in X''-axis (Tx'')

Remember that the equation of this force is:

$$T_x'' = F_x \cos\theta - \sin\theta (L \cos\alpha + (T - D) \sin\alpha) \quad (4.2.1.1)$$

In figure 40, the contribution of the first and second term of the equation 4.2.1.1 can be seen. This series is computed with  $\theta$  equal to  $30^\circ$  and wind speed equal to 10 m/s.

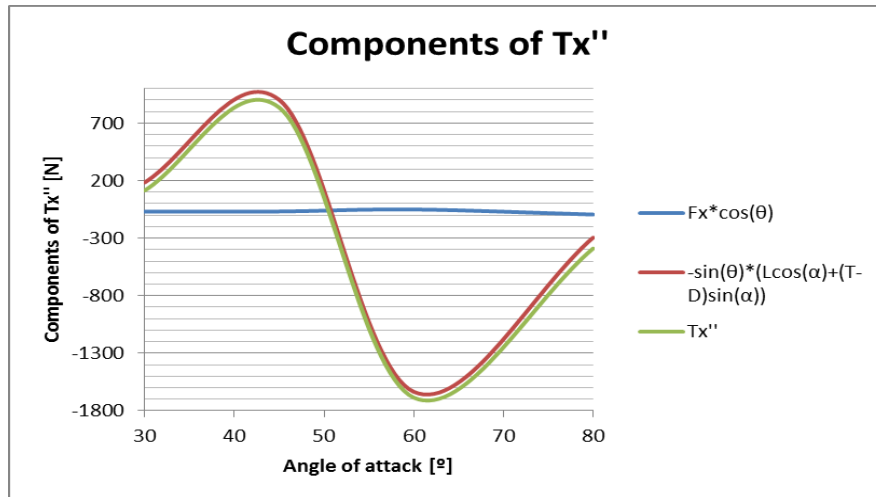


Figure 40. Components of  $T_x''$  depending on  $\alpha$  (wind speed = 10 m/s)

Figure 40 shows that the most important component to determine the  $T_x''$  is the second term, XY-Plane forces.

The reason of  $T_x''$  analysis is to know which are the limits of this force and which configurations can be used. In figure 41 and 42, some limits are taken into account. The rectangle remarks the non-realistic configurations. In order to sail in a stationary situation, the  $T_x''$  has to be negative. This force will provide grip to the board [19].

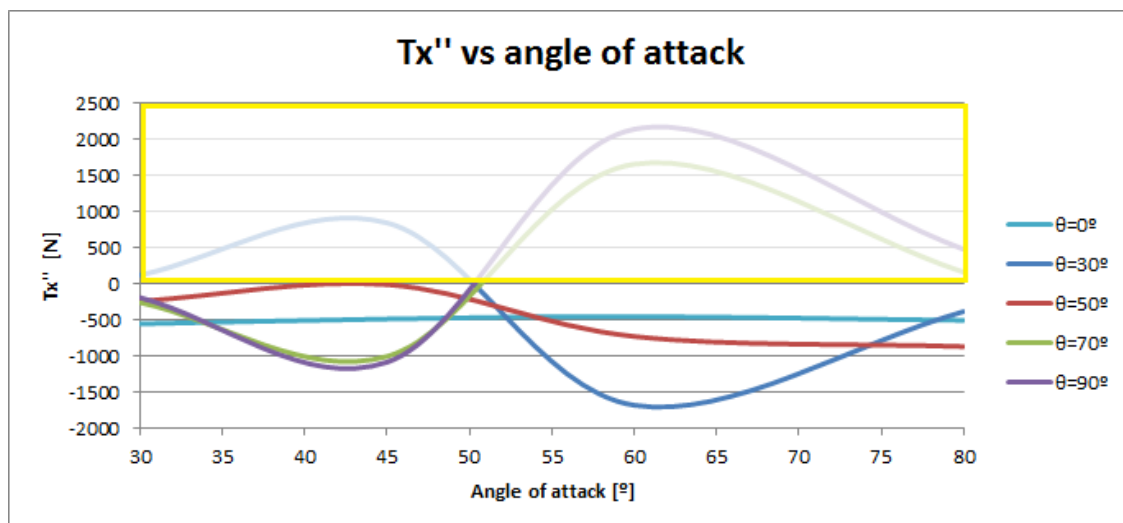


Figure 41.  $T_x''$  depending on  $\alpha$  and  $\theta$  (wind speed = 10 m/s)

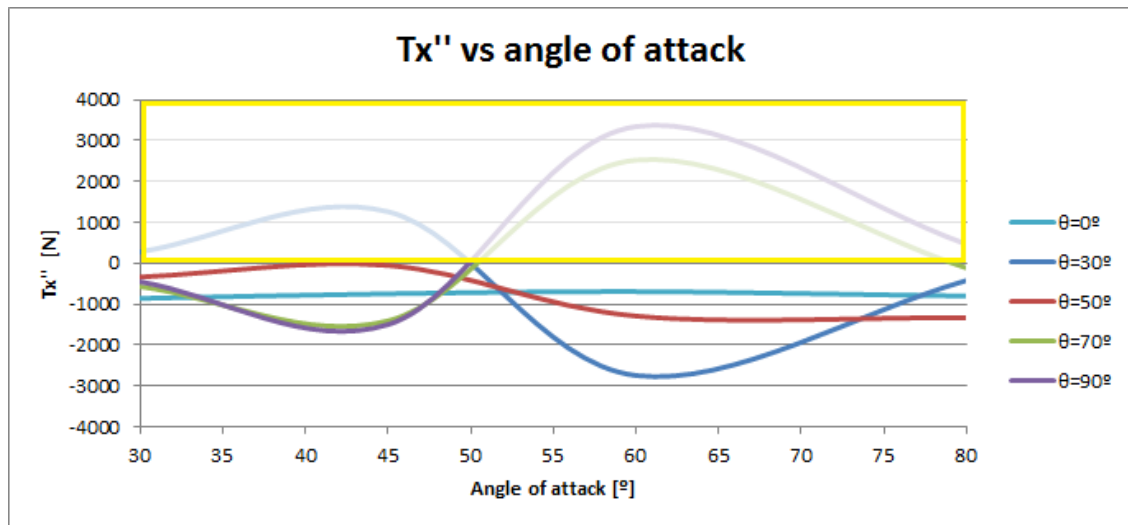


Figure 42.  $T_x''$  depending on  $\alpha$  and  $\theta$  (wind speed = 12 m/s)

This behaviour is due to the XY Plane term that there are two forces affecting the shape of this figure: lift and  $F_z$ . Lift increases when the  $\alpha$  increases, but it is multiplied by a cosinus that depends on  $\alpha$ .  $F_z$  has two peaks in  $45^\circ$  and  $60^\circ$  that can be seen in figures 41 and 42.  $F_z$  has multiplied a sinus that increases the term when  $\alpha$  increases. This is the reason why the second peak in  $T_x''$  graph is bigger than the first.

The possible configurations are independent of the wind speed. The only difference between figures 41 and 42 is the slope and values of the peaks reached.

Only when the inclination angle is  $30^\circ$  and  $50^\circ$ , all the angles of attack will be realistic. When  $\theta$  is  $70^\circ$  or more, the possible angles of attack are until  $50^\circ$ . On the contrary, when  $\theta$  is  $30^\circ$  the possible configurations are only from  $50^\circ$

#### 4.3.2 Force in Y''-axis ( $T_y''$ )

Remember that the equation of this force is:

$$T_y'' = F_x \sin \theta + (L \cos \alpha + (T - D) \sin \alpha) \cos \theta \quad (4.2.2.1)$$

In figure 35, is the same example as in figure 43 but in this case are the components for  $T_y''$ .

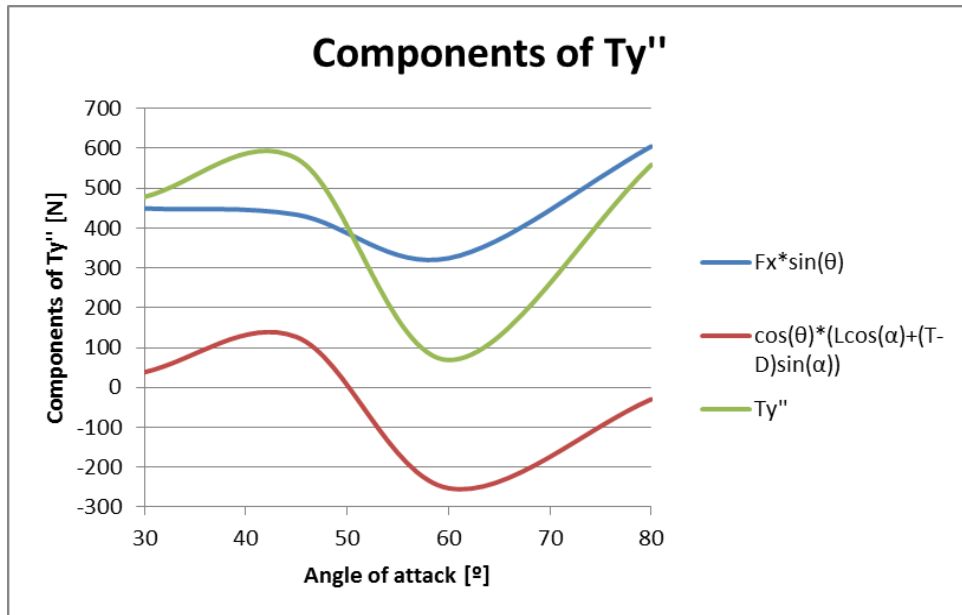


Figure 43. Components of  $Ty''$  depending on  $\alpha$  (wind speed = 10 m/s)

In this case, the behaviour is the opposite than in figure 40 when the contribution of the different aerodynamic forces is analysed.

As can be seen in figure 44 and 45,  $Ty''$  has to be at least positive. A more restrictive limit cannot be supposed because of the unknown value of the flotation force. Remember that the sum of the flotation force and  $Ty''$  balance the weight.

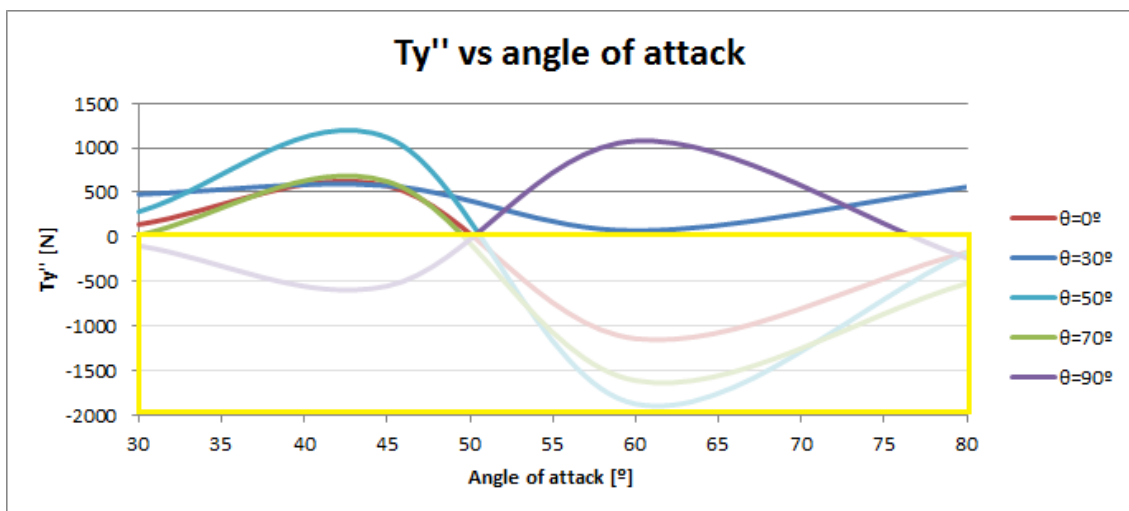


Figure 44.  $Ty''$  depending on  $\alpha$  and  $\theta$  (wind speed = 10 m/s)

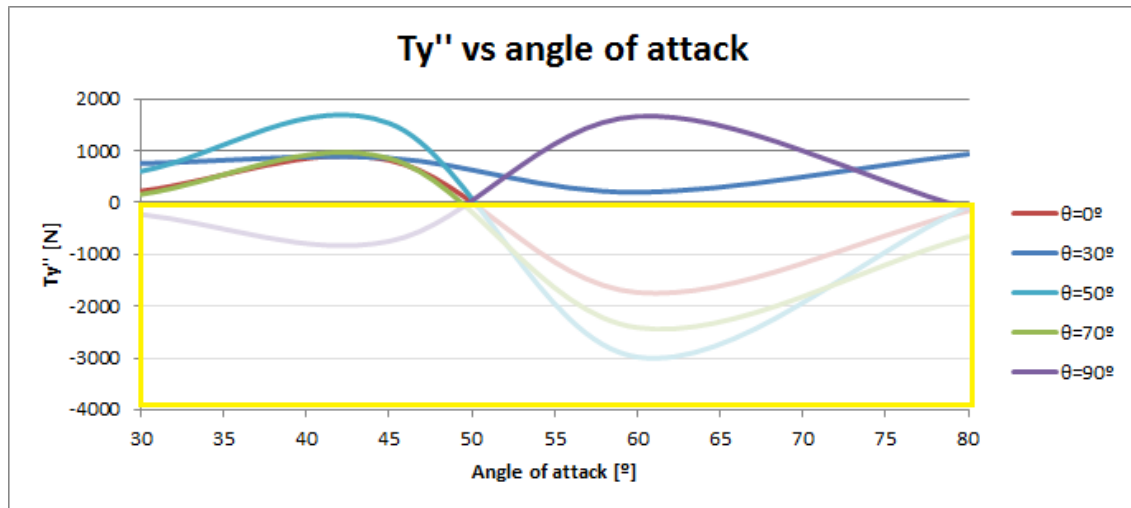


Figure 45.  $T_y''$  depending on  $\alpha$  and  $\theta$  (wind speed = 12 m/s)

The justification of the graphs shape is the same as in  $T_x''$ , because both graphs are derived from the same equations pattern. In this case, the first term,  $F_x$ , will have more influence on the graph.

The difference between figures 44 and 45 is the slope and the peak value, as happened in figures 41 and 42. But there is no difference in the possible configurations.

### 4.3.3 Force in Z''-axis ( $T_z''$ )

Remember that the equation of the  $T_z$  is:

$$T_z'' = L \sin \alpha - (T - D) \cos \alpha \quad (4.2.3.1)$$

To be in a stationary situation, the velocity of the kiter has to be constant. For that reason, the forces in Z''-axis has to be in equilibrium. So, the  $T_z$  and the board's drag have to be equal. Therefore, the only limitation of  $T_z$  is that has to be positive. This is represented in figures 46 and 47 for wind speed 10 m/s and 12 m/s, respectively.

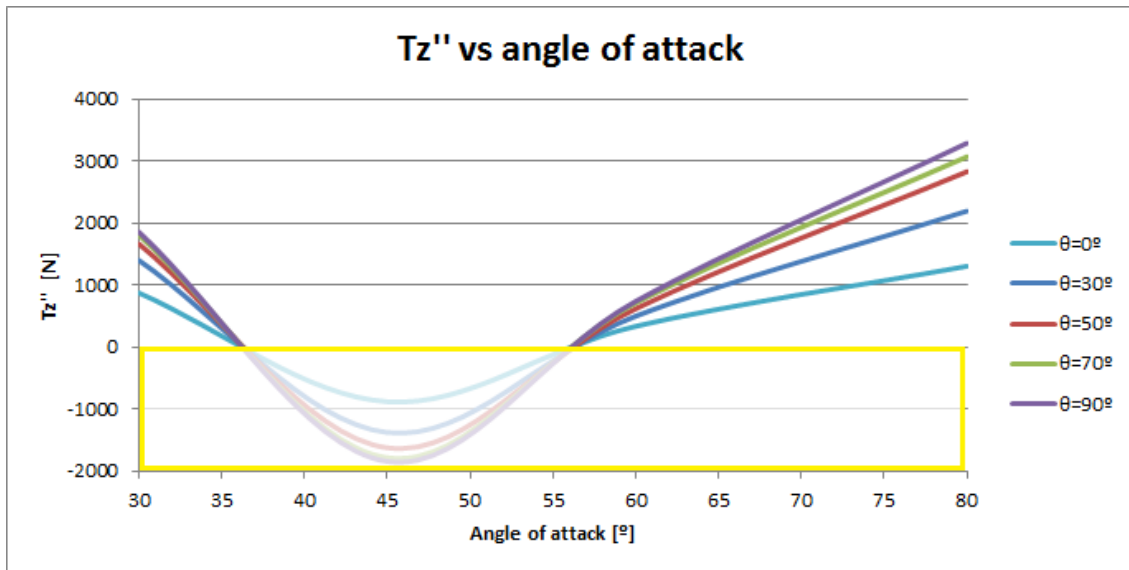


**Figure 46. Tz'' depending on  $\alpha$  and  $\theta$  (wind speed = 10 m/s)**

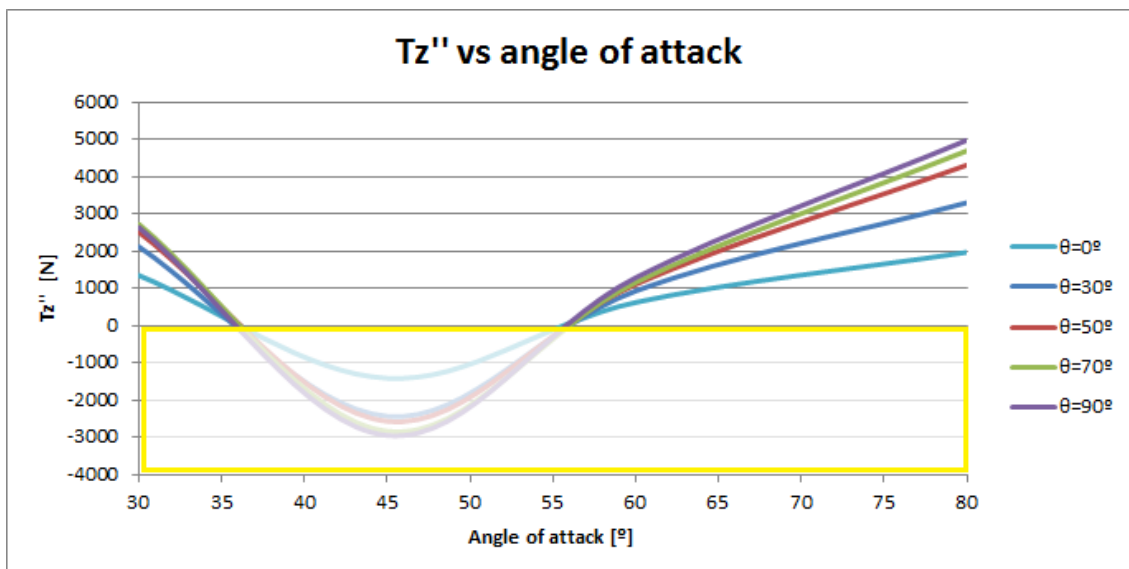


**Figure 47. Tz'' depending on  $\alpha$  and  $\theta$  (wind speed = 12 m/s)**

The shape for these graphs are easy to explain. When  $\alpha$  is small, the behaviour of  $F_z$  prevails, because of the sinus and cosinus that are multiplied the terms. After, the roles are changed and the lift prevails.

The limits are the same in both graphs, figures 46 and 47. But the peak values are a little less than the double.

### 4.3.4 Forces optimization

In summary, the possible configurations either in 10 m/s or 12 m/s speed are the shown in figure 48.

	$\alpha=30^\circ$	$\alpha=45^\circ$			$\alpha=60^\circ$		$\alpha=80^\circ$
$\theta=0^\circ$	√	X	X	X	X	X	X
$\theta=30^\circ$	X	X	X	X	√	√	√
$\theta=50^\circ$	√	X	X	X	X	X	X
$\theta=70^\circ$	√	X	X	X	X	X	X
$\theta=90^\circ$	X	X	X	X	X	X	X

Figure 48. Resume table of possible configurations

As a result, a low angle of attack is needed and the maximum inclination angle is  $70^\circ$ . In this situation,  $T_y''$  increases with the angle of attack, while  $T_z''$  decreases and  $T_x''$  doesn't affect on the performance.

In order to get the best configuration, there are two points to take in consideration. First,  $T_x''$  doesn't enhance noticeably the performance. Besides,  $T_y''$  and  $T_z''$  have to be a specific value to accomplish the equilibrium in  $Y''$  and  $Z''$ -axis.

The configuration that creates more  $T_y''$  is the  $\theta$  equal to  $30^\circ$  and  $\alpha$  equal to  $45^\circ$ . And there will be more board's drag as velocity rises. Supposing that the forces will be in equilibrium the more  $T_z''$ , the more velocity the kiter has. The configuration that gives the most  $T_z''$  is when  $\alpha$  is equal to  $30^\circ$ .

## CHAPTER 5. CONCLUSIONS

In order to characterize the aerodynamic behaviour of a kite, a analysis and a interpretation of the results have been done. The first part, the analysis, consists of knowing the performance of lift,  $F_z$  and  $F_x$  forces. The second one justifies the possible configurations of angles. It consists on studying how the angles influence the forces acting upon the kiter and their limitations.

Lift,  $F_z$  and  $F_x$  appears only when there is a combination of going perpendicular to the wind and the curvature of the leading edge.

The analysis helps to study how this situation and the curvature affect on the forces generated on the kite. It allows to confirm which forces acting upon the kite are significant and to know why they are generated. In the XY Plane the common lift produced by an airplane's airfoil is decomposed in two forces: the lift of the kite and  $F_x$ . That is due to the curvature of the leading edge. In exchange of some kite's power, the kiter can sail and create thrust itself. This is the reason why bow kites can obtain more power than C-kites: the design of the curvature; in bow kites are devised taking into account this drawback and providing more lifting area.

The behaviour of these forces is also explained. While Lift grows constantly with the increasing of  $\theta$ ,  $F_x$  decreases. In this case, when the resultant velocity of wind is computed, the component in Y-axis increases at the cost of the component in X-axis. Depending if the velocity prevails in Y-axis or in X-axis, the forces will be more important in one or another direction. The lift dependance of  $\alpha$  is the same as in any common airfoil, but  $F_x$  remains almost constant until  $60^\circ$ , after, falls. Besides,  $F_z$  increases when either of the variables increases. The reason of the behaviour of  $F_z$  is that the kite in the situations studied doesn't stall and the wake is relatively not turbulent.

The second part, the interpretation, is where the forces acting upon the kite are decomposed in the coordinate system of the kiter, X''Y''Z'' coordinate system. The shape of these forces is due to mainly two forces: the lift and  $F_z$ .  $T_x''$  and  $T_y''$  are affected by them, but the shape of  $F_z$  prevails. On the contrary,  $T_z''$  is affected when  $\alpha$  is low by  $F_z$ , but after by the lift. To understand the real effects of kite forces and know the realistic values of  $\alpha$  and  $\theta$ , some limits in  $T_x''$ ,  $T_y''$  and  $T_z''$  are necessary to be applied. The general configuration obtained is a low angle of attack for almost any of inclination angles. The configuration that gives the most  $T_z''$  is when  $\alpha$  is equal to  $30^\circ$ , although the configuration that gibes the most  $T_y''$  is when the  $\theta$  is equal to  $30^\circ$  and  $\alpha$  is equal to  $45^\circ$ .

The only change between the case of wind speed equal to 10 m/s and 12 m/s is that the forces upon the kiter would be higher. But the decision of the configuration would be the same if the weight increases properly. If not, the need of  $T_y''$  could be less and with a low inclination angle would be enough.

The most important thing to remark is the necessity to take real measures to confirm the suppositions made on this work, such as the ratio between the wind speed and kite speed, the flotation force and board's drag force, etc. It is crucial, to know the exactly range of the angle of attack to do a better aerodynamic model.

## CHAPTER 6. BILIOGRAPHY

- [1] <http://www.zonakitesurf.com/>
- [2] <http://repository.tudelft.nl/view/ir/uuid%3Acdece38a-1f13-47cc-b277-ed64fdda7cdf/>
- [3]
- [4] <http://www.britishkitesurfingassociation.co.uk/>
- [5] <http://adventure.howstuffworks.com/outdoor-activities/water-sports/kitesurfing.htm>
- [6] <http://repository.tudelft.nl/view/ir/uuid%3A9e8e2dae-639b-4fd6-b4bd-1318b37e60c2/>
- [7] <http://www.atlanticsurfco.co.za/articles/what-is-a-bow-kite/>
- [8] Domina Jalbert , US Patent 3131894
- [9] [http://lr.home.tudelft.nl/fileadmin/Faculteit/LR/Organisatie/Afdelingen\\_en\\_Leerstoelen/Afdeling\\_AEWE/Wind\\_Energy/Education/Masters\\_Projects/Proposed\\_Master\\_Projects/FinalReport.pdf](http://lr.home.tudelft.nl/fileadmin/Faculteit/LR/Organisatie/Afdelingen_en_Leerstoelen/Afdeling_AEWE/Wind_Energy/Education/Masters_Projects/Proposed_Master_Projects/FinalReport.pdf)
- [10] [http://www.lr.tudelft.nl/fileadmin/Faculteit/LR/Organisatie/Afdelingen\\_en\\_Leerstoelen/Afdeling\\_AEWE/Applied\\_Sustainable\\_Science\\_Engineering\\_and\\_Technology/Publications/doc/AIAA-2009-2338-2871\\_roland\\_verheul.pdf](http://www.lr.tudelft.nl/fileadmin/Faculteit/LR/Organisatie/Afdelingen_en_Leerstoelen/Afdeling_AEWE/Applied_Sustainable_Science_Engineering_and_Technology/Publications/doc/AIAA-2009-2338-2871_roland_verheul.pdf)
- [11] <http://www.flyozone.com/kitesurf/pl/products/kites/instinct-edge/materials/>
- [12] [http://machinedesign.com/BDE/materials/bdemat2/bdemat2\\_29.html](http://machinedesign.com/BDE/materials/bdemat2/bdemat2_29.html)
- [13] Thesaurus dictionary.
- [14] <http://www.britishkitesurfingassociation.co.uk/kitesurfing-guides/terminology.html>
- [15] <http://www.grc.nasa.gov/WWW/k-12/airplane/incline.html>
- [16] Blade 2009's manual
- [17] <http://www.kitesurfingschool.org/speed.htm>
- [18] Kite model of the program: Surfplan Kite Software Version 5.03.0.5
- [19] <http://www.britishkitesurfingassociation.co.uk/kitesurfing-guides/terminology.html>